

# **The novel reversible LSD1 inhibitor SP-2577 promotes anti-tumor immunity in SWItch/Sucrose-NonFermentable (SWI/SNF) complex mutated ovarian cancer**

Raffaella Soldi<sup>1</sup>, Tithi Ghosh Halder<sup>1</sup>, Alexis Weston<sup>1</sup>, Trason Thode<sup>1</sup>, Kevin Drenner<sup>1</sup>, Rhonda Lewis<sup>1</sup>, Mohan R. Kaadige<sup>1</sup>, Shreyesi Srivastava<sup>3</sup>, Sherin Daniel Ampanattu<sup>1</sup>, Ryan Rodriguez del Villar<sup>1</sup>, Jessica Lang<sup>2</sup>, Hariprasad Vankayalapati<sup>5</sup>, Bernard Weissman<sup>4</sup>, Jeffrey M. Trent<sup>2</sup>, William P.D. Hendricks<sup>2</sup> and Sunil Sharma<sup>1</sup>

<sup>1</sup>Applied Cancer Research and Drug Discovery, Translational Genomics Research Institute (TGen) of City of Hope, 445 N. 5th Street, Phoenix, AZ 85004

<sup>2</sup>Integrated Cancer Genomics Division, Translational Genomics Research Institute (TGen) of City of Hope, 445 N. 5th Street, Phoenix, AZ 85004

<sup>3</sup>HonorHealth Clinical Research Institute, 10510 N 92nd St Suite 200, Scottsdale, AZ 85258

<sup>4</sup>Department of Pathology and Laboratory Medicine, Lineberger Cancer Center, University of North Carolina, Chapel Hill, NC 27514

<sup>5</sup>Huntsman Cancer Institute, University of Utah, 2000 Circle of Hope, Salt Lake City, UT 84112, USA.

**Running title: SP-2577 and SWI/SNF mutated malignancies**

**To whom correspondence should be addressed: Dr. Sunil Sharma, Sunil Sharma, MD, FACP, MBA, Deputy Director, Clinical Sciences, Professor and Division Director, Applied Cancer Research and Drug Discovery, Translational Genomics Research Institute (TGen), 445 N. Fifth Street, Phoenix, AZ 85004; T: 602-343-8402; F: 602-916-0602; ssharma@tgen.org**

**Keywords: SWI/SNF, SCCOHT, LSD1, SP-2577, Immune response, Checkpoint inhibitors, Cancer therapy.**

## **Abstract**

Chromatin remodeling SWItch/Sucrose-NonFermentable (SWI/SNF) complexes, initially identified in yeast 20 years ago, are evolutionarily conserved multi-subunit protein complexes that

use the energy from hydrolysis of adenosine triphosphate (ATP) to remodel nucleosome structure and modulate transcription. Mutations in proteins of SWI/SNF complexes occur in 20% of human cancers including ovarian cancer (OC). Approximately 50% of ovarian clear cell carcinoma (OCCC) carries mutations in the SWI/SNF subunit ARID1A while small cell carcinoma of the ovary hypercalcemic type (SCCOHT) is driven primarily by genetic inactivation of the SWI/SNF ATPase SMARCA4 (BRG1) alongside epigenetic silencing of the homolog ATPase SMARCA2 (BRM). Dual loss of these ATPases disrupts SWI/SNF chromatin remodeling activity and may also interfere with the function of other histone-modifying enzymes that associate with or are dependent on SWI/SNF activity. One such enzyme is lysine-specific histone demethylase 1 (LSD1/KDM1A) which regulates the chromatin landscape and gene expression by demethylating proteins, including histone H3. LSD1 associates with epigenetic complexes such as the nucleosome remodeling deacetylase complex (NuRD) and SWI/SNF to inhibit the transcription of genes involved in tumor suppression and cell differentiation. TCGA analysis of human cancers shows that LSD1 is highly expressed in SWI/SNF-mutated tumors. Further, SCCOHT and OCCC cell lines show low nM IC<sub>50</sub>s for the reversible LSD1 inhibitor SP-2577 (Seclidemstat, currently in clinical phase I trials), supporting that these SWI/SNF-deficient ovarian cancers are dependent on LSD1 activity. Recently, it has been also shown that inhibition of LSD1 stimulates interferon (IFN)-dependent anti-tumor immunity through induction of Endogenous Retroviruses Elements (ERVs) and may thereby overcome resistance to checkpoint blockade. Additionally, SCCOHTs have been shown to exhibit an immune-active tumor microenvironment with PD-L1 expression in both tumor and stromal cells that strongly correlated with T cell infiltration. Thus, in this study we investigated the ability of SP-2577 to promote anti-tumor immunity and T cell infiltration in SWI/SNF-mutant SCCOHT and OCCC models. Our data shows that the reversible LSD1 inhibitor SP-2577 stimulates IFN-dependent anti-tumor immunity in SCCOHT cells *in vitro* in a 3D immune-organoid platform. Additionally, SP-2577 promoted the expression of PD-L1 in both SCCOHT and

OCCC models. Together our findings suggest that SP-2577 and checkpoint inhibitors as a therapeutic combination may induce or augment immunogenic responses in these tumors.

## Introduction

An increasing number of cancers are recognized to be driven partly by inactivation of subunits of the SWItch/Sucrose-NonFermentable (SWI/SNF) complex, a multi-protein ATP-dependent chromatin-remodeling complex with central roles in cell differentiation programs (1,2). Pathogenic SWI/SNF mutations occur across diverse adult cancers, typically in a genomic background of numerous other driver mutations and/or genomic instability (3,4). However, SWI/SNF driver mutations also occur in a unique subset of more uniform cancers, such as small cell carcinoma of the ovary hypercalcemic type (SCCOHT) (5), rhabdoid tumors (RT) (6,7), thoracic sarcomas (8,9), and renal medullary cancers (10). These cancers share genetic and phenotypic features even though they arise from different anatomic sites (1). Shared features include poorly differentiated morphology, occurrence in young populations, and clinically aggressive behavior (11,12). Their genetic makeup is relatively simple, with an overall low tumor mutation burden, few structural defects, and, in most cases, universal inactivation of a single subunit in the SWI/SNF complex. Particularly, in ovarian cancers (OCs), the most lethal gynecologic malignancies in the developed world and the fifth leading cause of cancer-associated mortality among women in the United States (13), SWI/SNF alterations vary in different histologic subtypes. The ARID1A (BAF250a) subunit is mutated in approximately 50% of ovarian clear cell carcinomas (OCCC) and 30% of ovarian endometrioid carcinomas (OEC) (14). SCCOHT (15), a rare and very aggressive OC, is a single-gene disease with inactivating mutations in the subunit SMARCA4 (BRG1) (16-18) and epigenetic silencing of SMARCA2 (BRM) expression (17). SCCOHT is the most common undifferentiated ovarian malignant tumor in women under 40 years. In contrast, OCCC targets women aged 55 years or older and is characterized by mutations in phosphatidylinositol-4, 5-bisphosphate 3-kinase catalytic subunit  $\alpha$  (PIK3CA) (19,20) and

phosphatase and tensin homolog (PTEN), in addition to the ARID1A mutations. Both SCCOHT and OCCC respond poorly to conventional chemotherapy, and to date there is no consensus on the optimal therapeutic strategy (5,20-23).

ATP-dependent chromatin remodeling plays a critical role in cell differentiation through control of transcriptional programs. When disrupted, these programs result in abnormal gene expression that creates therapeutically targetable oncogenic dependencies (24). For example, in BRG1-deficient non-small cell lung cancers, BRM has been identified as a candidate synthetic lethal target (25,26). Similarly, in BRG1-deficient small cell lung cancer, MYC-associated factor X (MAX) was identified as a synthetic lethal target (27). In ARID1A-mutated OC, inhibition of DNA repair proteins PARP and ATR, and the epigenetic factors EZH2, HDAC2, HDAC6 and BRD2 have all shown therapeutic promise (28). In SCCOHT, therapeutic vulnerabilities to receptor tyrosine kinase inhibitors (29), EZH2 inhibitors (30-32), HDAC inhibitors (33), bromodomain inhibitors (34), and CDK4/6 inhibitors (35,36) have also been identified. Importantly, correlations between SWI/SNF mutations and responses to immune checkpoint inhibitors have also been observed (37). In renal cell carcinoma, patients carrying mutations in bromodomain-containing genes (PBRM1 and BRD8) showed exceptional response to the anti-CTLA-4 antibody Ipilimumab (38). A CRISPR screen to identify genes involved in anti-PD-1 resistance identified three SWI/SNF complex members as important determinants in melanoma (39). A moderate response to anti-PD-1 treatment was also reported in a cohort of four SCCOHT patients expressing PD-L1 (40), suggesting that the low tumor mutation burden is not a limitation for checkpoint immunotherapy. OCCC models have also recently been described to be responsive to checkpoint inhibition in combination with HDAC6 inhibitors, particularly in the ARID1A-deficient setting (41). In a Phase II clinical trial testing Nivolumab in platinum-refractory ovarian cancers, one of the two OCCC patients demonstrated a complete response (42). These data suggest that novel treatment approaches and combinations should be adopted to develop targeted therapies against SWI/SNF-mutant ovarian cancers.

LSD1 is an epigenetic enzyme that can either repress target gene expression by demethylating mono- or di-methylated histone H3 lysine 4 (H3K4me1/2) or activate targets by removing repressive H3K9me1/2. LSD1 is implicated in tumorigenesis and progression of many cancers and high LSD1 levels frequently correlate with aggressive cancer features (43-45). LSD1 also promotes tumor progression through demethylation of non-histone substrates such as p53, E2F1, DNMT1, and MYPT1, a regulator of RB1 phosphorylation (46-50). Further, recent studies indicate that LSD1 ablation can trigger anti-tumor immunity through stimulation of expression of endogenous retroviral elements (ERVs) and downregulation of expression of the RNA-induced silencing complex (RISC). The accumulation of double-stranded RNA (dsRNA) results in the stimulation of interferon (IFN)  $\beta$ -dependent immunogenic responses (51). These studies also show that LSD1 inhibition overcomes resistance to checkpoint blockade therapy *in vivo* by increasing tumor immunogenicity and T cell infiltration (51-53). Several studies have shown interaction between LSD1 and SWI/SNF complexes. In glioma, LSD1 is part of a co-repressor complex containing TLX, RCOR2 and the SWI/SNF core complex. Together, this co-repressor complex regulates stem-like properties of glioma initiating cells (GICs) (54). When associated with SWI/SNF, CoREST, HDAC1/2 and DNMTs, LSD1 regulates gene expression in the neural network underlying neurodegenerative diseases and brain tumors (55). In breast cancer, LSD1 associates with the SWI/SNF subunit SMARCA4 to form a hormone-dependent transcriptional repressor complex (56). A similar association is required for endogenous Notch-target gene expression in T-ALL cells (57). These findings suggest LSD1 as an important therapeutic target in cancers driven by SWI/SNF mutations.

In this study, we explored the therapeutic potential of SP-2577 (Secclidemstat, Salarius Pharmaceuticals, Houston TX), a potent reversible LSD1 inhibitor currently in Phase I clinical trials for Ewing Sarcoma (NCT03600649) and for advanced solid tumors (NCT03895684), to promote anti-tumor immunity and T cell infiltration in SWI/SNF-mutant OC. Our findings show that SP-2577 promotes ERV expression, activates the dsRNA-induced IFN pathway, and enhances T

cell infiltration in SCCOHT. Treatment with SP-2577 also promotes PD-L1 expression, and thus can potentially overcome resistance to anti-PD-1 therapy in SCCOHT. Finally, the efficacy of SP-2577 to promote T cell infiltration is not exclusive to SCCOHT. We observed similar effects in other SWI/SNF mutation-dependent OCs, such as ARID1A-mutant OCCC. Our data strongly suggest LSD1 as a potential therapeutic target in SCCOHT and provides preclinical evidence supporting the combinatorial use of SP-2577 with anti-PD-L1 for SWI/SNF-mutation-dependent OCs.

## Results

### *LSD1 is highly expressed in SWI/SNF-mutant cancers and the LSD1 inhibitor SP-2577 inhibits SWI/SNF-mutation-dependent tumor cell proliferation*

TGCA analysis using cBioPortal showed that LSD1 is highly expressed in the majority of human cancers, including in SWI/SNF-mutant tumors (58,59) (Fig. 1 A and B). To determine the effects of SP-2577 on SWI/SNF-mutant cell viability, we performed drug-dose-response (DDR) studies with 72 h CellTiterGlo viability endpoints in SCCOHT (SMARCA4<sup>-/-</sup>), OCCC (ARID1A<sup>-/-</sup>), lung (SMARCA4<sup>-/-</sup>), kidney (SMARCB1<sup>-/-</sup>), and colorectal cancer cell lines (SMARCA4<sup>-/-</sup>). All cell lines were sensitive to the treatment and showed sub-micromolar IC<sub>50</sub>s (Table 1). SP-2513, an analog of SP-2577, which only poorly inhibits LSD1 enzymatic activity (Table 2), showed significantly higher 72 h IC<sub>50</sub>s that ranged from 3.5 to 10  $\mu$ M (Table 1).

### *Inhibition of LSD1 by SP-2577 promotes ERV expression and induces expression and release of effector T cell attracting chemokines in conditioned medium*

Inhibition of LSD1 activity has been suggested to enhance anti-tumor immunity through activation of ERVs and production of dsRNA, followed by activation of an IFN- $\beta$ -dependent immune response (51). To investigate whether SP-2577 treatment could promote a similar response in SCCOHT tumors, we analyzed the expression of ERVL, HERVK, and IFN- $\beta$  in

SCCOHT cell lines (COV434, BIN 67 and SCCOHT-1) treated with SP-2577. After 72 h treatment with 3 $\mu$ M SP-2577, quantitative PCR (qPCR) analysis showed that SP-2577 significantly upregulated the expression of ERVs, IFN- $\beta$ , and interferon-stimulated genes ISG15 and CXCL10, suggesting activation of an IFN-dependent immune response (Fig. 2A). Recently it has been shown that LSD1 inhibition in triple negative breast cancer cell lines induces expression of CD8<sup>+</sup> T cell-attracting chemokines including CCL5, CXCL9, and CXCL10 (60). The expression of these genes along with PD-L1 was shown to have increased H3K4me2 levels at proximal promoter regions (60) in response to LSD1 inhibition. To determine whether SCCOHT cell lines release CD8<sup>+</sup> T cell-attracting chemokines after LSD1 inhibition, we analyzed the conditioned media from COV434 cells treated with SP-2577 for 72 h. Our U-PLEX MSD data showed that treatment with SP-2577 stimulated chemokine secretion in COV434 culture medium (Fig. 2B). Further, secretion of cytokines including IL-1 $\beta$ , IL-2, and IL-8 were also observed in the treated conditioned medium. Together, these data suggest that SP-2577 may play a role in the promotion of anti-tumor immunity.

#### *SP-2577 promotes lymphocyte infiltration in 3D culture of SCCOHT cell lines*

To examine whether SP-2577-dependent cytokine and chemokine secretion could enhance lymphocyte trafficking and tumor infiltration, we carried out an *ex vivo* migration/infiltration assay. SCCOHT cell lines COV434, BIN67, and SCCOHT-1 were grown in low concentration matrigel to form 3D organoids. To prevent SP-2577 cytotoxic damage from directly impacting cell viability, the organoids were cultured in conditioned media from SCCOHT cell lines collected 72 h post-treatment with SP-2577. At this time point there was no drug present in the conditioned medium. Migration and infiltration of lymphocytes was determined utilizing RFP-stained human allogeneic PBMCs. PBMCs were added to organoid cultures and migration toward the organoids was assessed by three dimensional Z-stack imaging and morphometric analysis (Cytation 5, BIOTECK). SP-2577 promoted PBMC infiltration in organoids more

efficiently than the less active analog SP-2513 (Fig. 3A). Immunofluorescence analysis further demonstrated the presence of stained PBMCs in the sectioned organoids that were treated with SP-2577 conditioned medium while they were absent in organoids cultured in SP-2513 or DMSO-conditioned medium (Fig. 3B). Finally, to determine the dependency of PBMC infiltration on SP-2577, we performed *ex vivo* migration/infiltration studies with higher concentrations of the LSD1 inhibitor (0.03 -3 $\mu$ M). SP-2577 induced PBMC infiltration into the SCCOHT organoids in a dose-dependent manner (Fig. 3C). Together, these observations suggest that the chemokines and cytokines secreted by SCCOHT cells in response to SP-2577 treatment promote the migration and infiltration of PBMCs in tumor organoids.

#### *Inhibition of LSD1 by SP-2577 induces expression of PD-L1*

LSD1 expression has been shown to negatively correlate with expression of immune-related genes including PD-L1 (60). Further, LSD1 has been shown to play a critical role in epigenetic silencing of the expression of PD-1 (61) and LSD1 inhibition results in increased expression of PD-L1 in tumor cells (51,60). To investigate the effect of SP-2577-dependent LSD1 inhibition on the expression of PD-L1 in SCCOHT, we treated COV434 organoids with 3  $\mu$ M SP-2577 and performed qPCR analysis for PD-L1 expression. We observed a significant increase in PD-L1 expression (Fig. 4A). Next, we tested if checkpoint blockade could amplify the immune cell infiltration effect in the presence of SP-2577 in immune-organoids. As shown in figure 4B, co-treatment of low doses (100 nM) of SP-2577 with  $\alpha$ -PD-L1 significantly increased lymphocyte infiltration. Moreover, the combination of  $\alpha$ -PD-L1 and  $\alpha$ -CTLA-4 was able to significantly enhance the infiltration of PBMCs in the SP-2577-treated COV434 organoids (Fig. 4B).

#### *SMARCA4 re-expression in SCCOHT cell lines blocks lymphocyte infiltration*

Although SCCOHT is characterized by low tumor mutation burden, recent studies have indicated that the tumor microenvironment of SCCOHT is similar to other immunogenic tumors

that respond to checkpoint blockade (37,40,62), suggesting that mutations in the subunits of the SWI/SNF complex may contribute to immunotherapy sensitivity. We questioned whether the restoration of SWI/SNF functionality in SCCOHT would affect the lymphocyte trafficking and tumor infiltration observed with SP-2577 treatment. To investigate this hypothesis, we used an isogenic COV434 cell line (COV434 pIND20 BRG1 2.7) where SMARCA4 (*BRG1*) was re-expressed under a doxycycline inducible system (29). qPCR and Western blotting analysis confirmed the expression of SMARCA4 in doxycycline-treated cells (Fig. 5A, B). SMARCA2 (*BRM*), which is normally silent in SCCOHT tumors, was also overexpressed by 14-fold after BRG1 induction (Fig. 5B). We observed a significant reduction in the level of infiltrated lymphocytes in SMARCA4 re-expressed organoids after SP-2577 treatment (Fig. 5C). Remarkably, expression of ERVL, HERVK, IFN $\beta$ , as well as interferon-stimulated genes ISG15 and CXCL10 was significantly downregulated in SMARCA4-induced cells after treatment with SP-2577 (Fig. 5D). In addition, re-expression of SMARCA4 resulted in downregulation of PD-L1 expression in SCCOHT cell lines (Fig. 5E). Lastly, the production and secretion of cytokines and chemokines that were induced by SP-2577 treatment were negatively affected by the re-expression of SMARCA4 in SCCOHT cells (Fig. 5F).

To determine if the reduction of lymphocyte infiltration was solely dependent on the re-expression of SMARCA4, we cultured doxycycline treated COV434 pIND20 BRG1 2.7 organoids with conditioned medium generated from SP-2577-treated parental SCCOHT cells lacking SMARCA4 expression. As shown in Fig. 5G, the presence of cytokines and chemokines in SP-2577-treated conditioned medium was not sufficient to overcome the impaired infiltration of lymphocytes in SMARCA4-expressing organoids, suggesting that SMARCA4-dependent epigenetic changes may have altered the immunogenicity of the organoids.

*SP-2577 promotes lymphocyte infiltration in ARID1A deficient cells*

To investigate if SP-2577 promotes tumor immune response in other SWI/SNF-mutant tumor types, we performed *ex vivo* migration and infiltration of lymphocytes in ARID1A-deficient OCCC cells. These studies were conducted in isogenic TOV21G cells, which re-express ARID1A under the control of doxycycline treatment. As previously observed in SCCOHT cell lines, SP-2577 promotes lymphocyte infiltration in a dose-dependent manner in parental TOV21G organoids (Fig. 6A). Re-expression of ARID1A resulted in a significant reduction in infiltration of lymphocytes (Fig. 6B). In addition, the combination of  $\alpha$ -PD-L1 and  $\alpha$ -CTLA-4 was able to significantly enhance the infiltration of PBMCs in the low dose (300 nM) SP-2577-treated parental TOV21G organoids (Fig. 6C).

## Discussion

SWI/SNF complexes have previously been implicated in regulation of the immune system, particularly in enhancing interferon-stimulated gene (ISG) expression (63) through a STAT-dependent mechanism. However, it has been reported that inactivating mutations in SWI/SNF subunits (ARID1A, PBRM1, SMARCB1, and SMARCA4) also sensitize cancer cells to T cell-mediated destruction (37). SWI/SNF loss-of-function enhances the expression of immune checkpoint regulators and neoantigen presentation (37,39,64). Even monogenic tumors like SCCOHTs are immunogenic and exhibit biologically significant levels of T cell infiltration and PD-L1 expression (40). It has been reported that several patients with mutations in the SWI/SNF complex have benefited from checkpoint blockade immunotherapy (37,39,40). Although immune checkpoint inhibitor treatment has shown promising results, only a minority of treated patients exhibit durable responses (40,65). Additionally, many of those who initially respond to treatment eventually experience relapse due to acquired resistance. As with conventional cancer therapies, one way to improve clinical responses with immune checkpoint blockade is through combination therapy strategies.

Numerous studies have revealed that epigenetic modulation plays a key role in tumor immune escape. Cancer cells show frequent loss or epigenetic silencing of the cytosolic DNA sensor cGAS and/or STING to promote immune evasion (66). Conversely, aberrant LSD1 activity suppresses the expression of immune protective factors (60) such as PD-L1 and CTLA-4. Recently, it has been shown that inhibition of LSD1 significantly increases tumor immunogenicity (51) primarily through changes in methylation levels. An increased methylation level promotes endogenous retroviral (ERV) expression, leading to dsRNA stress. Methylation of the RISC complex member AGO2 results in destabilization of the integrity of complex and inhibition of dsRNA degradation. dsRNA stress activates IFN-dependent immune response that consequently sensitizes tumors to T cell immunity and T cell infiltration. As LSD1 is highly expressed in SCCOHT cell lines and interacts with members of the SWI/SNF complex to regulate gene expression (55,67,68), it is an ideal therapeutic target for the treatment of SCCOHT and potentially other SWI/SNF loss of function- dependent cancers.

In this study, we demonstrate that inhibition of LSD1 activity by the reversible inhibitor SP-2577 (Secclidemstat) induces the expression of ERVs and IFN $\beta$  in SCCOHT. In agreement with the previous observation that LSD1 negatively regulates expression of chemokines and immune protective factors such as PD-L1 (60), inhibition of LSD1 with SP-2577 promoted expression of chemokines and PD-L1 in SCCOHT cell lines, which results in activation of T cell infiltration.

The contribution of ERVs to the immune response is not limited to the dsRNA/MDA5 interaction followed by activation of the IFN pathway. Tumor neoantigen analysis has shown that ERVs can encode for strictly tumor-specific antigens, otherwise silent in normal tissue, capable of eliciting T cell specific antitumor immunity. Schiavetti et al have shown that ERV-K antigens are highly expressed in a variety of malignancies such as breast, melanoma, sarcoma, lymphoma, and bladder cancer (69), and the ERV-E encoded antigen is selectively expressed in RCC kidney tumors (70). Moreover, it has been shown that in epithelial ovarian cancer and in colon cancer high levels of ERVs expression correlates robustly to immune checkpoint therapy response

(71,72). Expression of ERV elements is subjected to genome-wide regulation by epigenetic silencing (73,74). However, many ERVs are still transcribed in adult cells and contribute to autoimmune pathologies such as systemic lupus erythematosus and Aicardi–Goutières syndrome (75). Similarly, dysregulation of epigenetic pathways also contributes to reactivation of ERV elements in tumor cells (76).

SWI/SNF may play a role in the establishment of ERV silencing. In embryonic stem cells SMARCAD1, a SWI/SNF-like chromatin remodeler, negatively regulates the retrotransposon activity through recruitment of KRAB associated protein 1 (KAP1) (77). Docking KAP1 at the ERV elements in the genome triggers the formation of a complex with the histone methyltransferase SETDB1, resulting in formation of H3K9me3 and silencing of ERV class I and II. Lack of SMARCAD1 compromises the stability of KAP1-SETDB1 association at ERVs, which lead to reduction of H3K9me3 and activation of ERV transcription. Restoration of SMARCAD1 activity reverses the ERV upregulation (77). Similarly, SWI/SNF complex members, including SMARCA4 and LSH1, are known to ensure silencing of retrotransposons in the stem cells through interaction with DNMT3a and HDACs (74,77). Transcriptome analysis of rhabdoid tumors cell lines with inducible SMARCB1 re-expression identified significant ERVs overexpression in SMARCB1-deficient conditions (78). In support of this, our studies show that re-expression of SMARCA4 in SCCOHT or ARID1A in OCCC results in the loss of ERV expression and reduction of T cell infiltration, even in the presence of conditioned medium enriched in cytokines and chemokines, implying that T cell infiltration may be related to the loss of SWI/SNF complex function. Together these results suggest that SWI/SNF deficiency plays a crucial role on ERVs epigenetic silencing, resulting in enhancement of tumor immunogenicity. Moreover, LSD1-dependent histone modifications result in significant downregulation of ERVs (73,79). By inhibiting LSD1, SP-2577 ensures increased ERV activation and cytokine production, resulting in enhanced T cell immune response. In addition, SP-2577 treatment promotes PD-L1 expression, and co-treatment

with  $\alpha$ -PD-L1 or  $\alpha$ -CTLA-4 antibodies significantly amplifies the T cell infiltration in SCCOHT and OCCC immune organoids.

Collectively, these findings demonstrate the important role of SP-2577 in the regulation of T cell recruitment to the tumor microenvironment and highlight the potential of combining SP-2577 with checkpoint immunotherapy in SCCOHT, OCCC, and other SWI/SNF mutated malignancies.

## **Materials and Methods**

### **Cell Lines and 2D Culture Maintenance**

SCCOHT cell lines BIN67 and SCCOHT-1 (Generously donated by Dr. William Hendrick, TGen) were cultured in RPMI Medium 1640 with L-Glutamine (Gibco) and supplemented with 10% FBS (Gibco) and 1% penicillin/streptomycin (Gibco). SCCOHT cell line COV434 (Generously donated by Dr. William Hendricks, TGen), OCCC cell line TOV21G (ATCC), and the doxycycline-inducible COV434 pIND20 BRG1-2.7 and TOV21G pIND20 ARID1A (generously donated by Dr. Bernard Weissman, University of North Carolina) were cultured in DMEM (Gibco) and supplemented with 10% TET free FBS (Corning) and 1% penicillin/streptomycin (Gibco). All cells were maintained at 37°C in a humidified incubator containing 5% CO<sub>2</sub>. All cell lines were routinely monitored for mycoplasma testing and STR profiled for cell line verification.

### **The LSD1 screening biochemical assay**

The LSD1 screening biochemical assay was performed as previously described (Sorna). Briefly, the LSD1 biochemical kit was purchased from Cayman Chemical (Ann Arbor, MI). SP-2577 and SP-2513 were diluted to 20X the desired test concentration in 100% DMSO and 2.5  $\mu$ L of the diluted drug sample was added to a black 384-well plate. The LSD1 enzyme stock was diluted 17-fold with assay buffer and 40  $\mu$ L of the diluted LSD1 enzyme was added to the appropriate wells. Substrate, consisting of horseradish peroxidase, dimethyl K4 peptide corresponding to the first 21 amino acids of the N-terminal tail of histone H3, and 10-acetyl-3, 7-dihydroxyphenoxazine was then added to wells. Resorufin was analyzed on an Envision plate reader with an excitation wavelength of 530 nm and an emission wavelength of 595 nm.

### **Cell Viability Assay**

Cells were seeded in 96-well plates in triplicate at a density of 500 to 2,000 cells per well depending on the growth curve of each cell line. 24 h later, cells were treated with DMSO, LSD1 inhibitor SP-2577, or analog SP-2513 at increasing concentrations (0.001 to 10  $\mu$ M). Cell viability was assessed with CellTiter-Glo (Promega) 72 h after treatment and IC<sub>50</sub>s were calculated using GraphPad Prism 8.0.

## Organoid Generation

SCCOHT cell lines (BIN67, SCCOHT-1, COV434) and the OCCC cell line TOV21G were seeded at 5000 cells per well in 96 well ultra-low attachment treated spheroid microplates (Corning) with the appropriate phenol red free medium containing 1.5% matrigel (Corning). Cells were maintained in culture for 72 h to generate spheroids for use in immune infiltration assays.

## Immune Infiltration Assay

### *SP-2577/SP-2513 Conditioned Media:*

The SCCOHT and OCCC cell lines were seeded in T-25 tissue culture treated flasks (Thermo Fisher) at  $3 \times 10^5$  cells in 5mL of the appropriate phenol red free complete growth medium. After 48 h, at 70-80% confluency, the cells were treated with  $3\mu\text{M}$  or  $1\mu\text{M}$  of SP-2577 or SP-2513. After 72 h, the media was collected from the flasks and stored at  $-80^\circ\text{C}$  until use in the infiltration assays.

### *Labeling PBMCs with RFP:*

Peripheral blood mononuclear cells (PBMC) (Lonza) were maintained in CTS OpTmizer T Cell expansion SFM (Thermo Fisher) in a T-75 suspension flask (Genesee Scientific) for 24 h at  $37^\circ\text{C}$ . After 24 h, cells were collected and washed with PBS (Gibco) and counted. Approximately  $2.5 \times 10^6$  PBMCs were labeled with Molecular Probes Vybrant CM-Dil Cell Labeling Solution (RFP)(Invitrogen) by incubating the PBMCs with a  $2\mu\text{M}$  solution of CM-Dil for 45 min at  $37^\circ\text{C}$  in the dark and then for an additional 15 min at  $4^\circ\text{C}$ . After the incubation, cells were washed with PBS twice and resuspended in the appropriate complete growth medium.

### *Checkpoint blockade:*

The following monoclonal blocking antibodies (final concentration  $10\mu\text{g/mL}$ ) were used for checkpoint blocking on tumors as well as T cells: functional grade PD-L1 (29E.2A3) and CTLA-4 (BN13) (Bioxcell, USA). In brief,  $2 \times 10^6$  PBMCs were treated with  $10\mu\text{g/mL}$  of  $\alpha\text{-CTLA-4}$  antibody and incubated at  $37^\circ\text{C}$  incubator for 45 min on shaker. Then the cells were washed in serum free media and stained with Molecular Probes Vybrant CM-Dil Cell Labeling Solution as mentioned above. Alternatively, COV434 tumor organoids were incubated with  $10\mu\text{g/mL}$  of  $\alpha\text{-PD-L1}$  antibody and incubated at  $37^\circ\text{C}$  incubator for 1h. Then the media containing  $\alpha\text{-PD-L1}$  was removed carefully and fresh conditioned media was added on all organoids.

### *Immune infiltration and imaging:*

$150\mu\text{L}$  of SP-2577 conditioned medium was added to each well containing a spheroid. A  $5\mu\text{m}$  HTS Transwell-96 Well permeable support receiver plate (Corning) was placed on each ultra-low attachment spheroid microplate (Corning) to allow for PBMC infiltration into the tumoroids. RFP-stained PBMCs were then seeded into inserts at  $5 \times 10^5$  cells/well to ensure tumoroid:PBMC cell ratio of 1:10. After 48 h, inserts were removed, and organoid microplates were analyzed by 3D Z-

stack imaging and morphometric analysis with Cytation 5 software to quantify the lymphocyte infiltration.

## **qPCR**

COV434, BIN67, and SCOOHT-1 cells were seeded at a  $1 \times 10^6$  cells in 2 mL in 6-well tissue culture treated plates (Corning). After 24 hrs, cells were treated with 1  $\mu$ M and 3  $\mu$ M of SP-2577 as well as 3 $\mu$ M of SP-2513 for 72 h. DMSO was used as negative control. To quantify gene expression, total RNA was extracted (Qiagen RNeasy Mini Kit) and quantified by spectroscopy (Nanodrop ND-8000, Thermo Scientific). Samples were then reverse transcribed to cDNA using a high capacity cDNA reverse transcription kit (Applied Biosystems) and the MJ Research thermal cycler. cDNA was amplified, detected, and quantified using SYBR green reagents (Applied Biosystems) and the ViiA 7 Real-Time PCR System (Applied Biosystems). Data were normalized to GAPDH expression. List of primers used in this study are listed in Supplemental section.

## **Fluorescent staining and imaging of Organoid**

Organoids grown in Matrigel were initially fixed in 4% PFA for 1.5 h. After PBS washing, organoids were embedded in Histogel, processed with an automated tissue processor (Tissue-Tek VIP), and embedded into a paraffin block (Tissue-Tek TEC). Samples were sectioned at 4  $\mu$ m onto poly-L-lysine coated slides and air-dried at room temperature overnight for any subsequent immunofluorescence staining. All slides for fluorescence were deparaffinized and antigen retrieved in pH 6 citrate buffer for a total of 40 min. After protein blocking, nuclei were stained with DAPI (Sigma). Infiltrating PBMCs were pre-stained with RFP as described previously. Imaging was performed on a Zeiss LSM880 fluorescent microscope with Zen Black software.

## **Western Blot**

COV434 pIND20 BRG1-2.7 cells were plated in 6 well tissue culture plates at a density of  $5 \times 10^5$  cells per well and left to adhere overnight. Once adherent, cells were treated with 1 $\mu$ M doxycycline (SIGMA) daily for 8 days. Cells were harvested daily and proteins were extracted from cell lysates and immunoblotted for SMARCA4 expression.

## **TCGA analysis**

TCGA PanCancer Atlas data was downloaded from cBioPortal. To identify SWI/SNF cancers cBioPortal was used to query samples with SMARCA4, ARID1A, SMARCB1, SMARCC1, and KDM1A mutations. Samples were removed that had only KDM1A mutations, KDM1A deletions, no profiling of SWI/SNF genes, or did not have expression data. Expression of KDM1A was plotted using RStudio.

## **U-PLEX MSD analysis**

MSD analysis was performed following manufacturer protocol. Briefly, conditioned media (CM) from SP-2577 and DMSO treated cells were collected and centrifuged at 1500 RPM for 5 min at 4°C to eliminate cell debris. CM was then concentrated using Centricon 10 KDa (Sigma) and 25

μL of the resulting CM was added in each well in the MSD plate (KIT #K15067L-2) and analyzed using Discovery Workbench 4.0 software.

### Statistical analysis

Student's T-tests were performed using GraphPad Prism 8.0. Symbols for significance: NS, non significant; \*= $p < 0.05$ ; \*\*= $p < 0.01$ ; \*\*\*\*= $p < 0.0001$ . All the *in vitro* experiments were performed in triplicate and repeated at least three times.

**Conflict of interest:** Dr. Sunil Sharma declares a financial interest in other companies doing research in cancer: Clinical research funding from Novartis, GSK, Millennium, MedImmune, Johnson & Johnson, Gilead Sciences, Plexxikon, Onyx, Bayer, Blueprint Medicines, XuanZhu, Incyte, Toray Industries, Celgene, Hengrui Therapeutics, OncoMed, Tesaro, AADi, Merck, Inhibrx Inc, AMAL Therapeutics, and Syndax. Equity from LSK BioPharma, Salaris Pharmaceuticals, Iterion Therapeutics, Proterus Therapeutics, ConverGene, and Stingray Therapeutics. Honoraria from Exelixis, Loxo Oncology, Natera Inc, Hengrui Therapeutics, Tarveda Therapeutics, Dracen Pharmaceuticals, and Barricade Therapeutics.

Dr. Raffaella Soldi holds stock in Salaris Pharmaceuticals.

The other authors declare that they have no conflict of interest with the contents of this article.

### Author contributions:

RS, TGH, AW and RRdV conducted the experiments, analyzed the results, and wrote most of the paper. KD performed the TGCA analysis. HV, MRK and WPDH provided advice on experimental design, interpretation of results and preparation of the manuscript. TT, RL, SHS, SDA, JL, BW and JMT provided advice on the preparation of the manuscript. SS conceived the idea for the

project, provided advice on experimental design, interpretation of results and preparation of the manuscript.

## References

1. St Pierre, R., and Kadoch, C. (2017) Mammalian SWI/SNF complexes in cancer: emerging therapeutic opportunities. *Curr Opin Genet Dev* **42**, 56-67
2. Williams, G. M., Hume, D. M., Hudson, R. P., Jr., Morris, P. J., Kano, K., and Milgrom, F. (1968) "Hyperacute" renal-homograft rejection in man. *N Engl J Med* **279**, 611-618
3. Brownlee, P. M., Meisenberg, C., and Downs, J. A. (2015) The SWI/SNF chromatin remodelling complex: Its role in maintaining genome stability and preventing tumourigenesis. *DNA Repair (Amst)* **32**, 127-133
4. Dutta, A., Sardu, M., Gogol, M., Gilmore, J., Zhang, D., Florens, L., Abmayr, S. M., Washburn, M. P., and Workman, J. L. (2017) Composition and Function of Mutant Swi/Snf Complexes. *Cell Rep* **18**, 2124-2134
5. Lu, B., and Shi, H. (2019) An In-Depth Look at Small Cell Carcinoma of the Ovary, Hypercalcemic Type (SCCOHT): Clinical Implications from Recent Molecular Findings. *J Cancer* **10**, 223-237
6. Agaimy, A., Daum, O., Markl, B., Lichtmanegger, I., Michal, M., and Hartmann, A. (2016) SWI/SNF Complex-deficient Undifferentiated/Rhabdoid Carcinomas of the Gastrointestinal Tract: A Series of 13 Cases Highlighting Mutually Exclusive Loss of SMARCA4 and SMARCA2 and Frequent Co-inactivation of SMARCB1 and SMARCA2. *Am J Surg Pathol* **40**, 544-553
7. Ramalingam, P., Croce, S., and McCluggage, W. G. (2017) Loss of expression of SMARCA4 (BRG1), SMARCA2 (BRM) and SMARCB1 (INI1) in undifferentiated carcinoma of the endometrium is not uncommon and is not always associated with rhabdoid morphology. *Histopathology* **70**, 359-366
8. Matsushita, M., and Kuwamoto, S. (2018) Cytologic Features of SMARCA4-Deficient Thoracic Sarcoma: A Case Report and Comparison with Other SWI/SNF Complex-Deficient Tumors. *Acta Cytol* **62**, 456-462
9. Yoshida, A., Kobayashi, E., Kubo, T., Kodaira, M., Motoi, T., Motoi, N., Yonemori, K., Ohe, Y., Watanabe, S. I., Kawai, A., Kohno, T., Kishimoto, H., Ichikawa, H., and Hiraoka, N. (2017) Clinicopathological and molecular characterization of SMARCA4-deficient thoracic sarcomas with comparison to potentially related entities. *Mod Pathol* **30**, 797-809
10. Pawel, B. R. (2018) SMARCB1-deficient Tumors of Childhood: A Practical Guide. *Pediatr Dev Pathol* **21**, 6-28
11. Biegel, J. A., Busse, T. M., and Weissman, B. E. (2014) SWI/SNF chromatin remodeling complexes and cancer. *Am J Med Genet C Semin Med Genet* **166C**, 350-366
12. Masliah-Planchon, J., Bieche, I., Guinebreteire, J. M., Bourdeaut, F., and Delattre, O. (2015) SWI/SNF chromatin remodeling and human malignancies. *Annu Rev Pathol* **10**, 145-171
13. Torre, L. A., Trabert, B., DeSantis, C. E., Miller, K. D., Samimi, G., Runowicz, C. D., Gaudet, M. M., Jemal, A., and Siegel, R. L. (2018) Ovarian cancer statistics, 2018. *CA Cancer J Clin* **68**, 284-296

14. Kadoch, C., Hargreaves, D. C., Hodges, C., Elias, L., Ho, L., Ranish, J., and Crabtree, G. R. (2013) Proteomic and bioinformatic analysis of mammalian SWI/SNF complexes identifies extensive roles in human malignancy. *Nat Genet* **45**, 592-601
15. Fukumoto, T., Magno, E., and Zhang, R. (2018) SWI/SNF Complexes in Ovarian Cancer: Mechanistic Insights and Therapeutic Implications. *Mol Cancer Res* **16**, 1819-1825
16. Jelinic, P., Mueller, J. J., Olvera, N., Dao, F., Scott, S. N., Shah, R., Gao, J., Schultz, N., Gonen, M., Soslow, R. A., Berger, M. F., and Levine, D. A. (2014) Recurrent SMARCA4 mutations in small cell carcinoma of the ovary. *Nat Genet* **46**, 424-426
17. Karnezis, A. N., Wang, Y., Ramos, P., Hendricks, W. P., Oliva, E., D'Angelo, E., Prat, J., Nucci, M. R., Nielsen, T. O., Chow, C., Leung, S., Kommoss, F., Kommoss, S., Silva, A., Ronnett, B. M., Rabban, J. T., Bowtell, D. D., Weissman, B. E., Trent, J. M., Gilks, C. B., and Huntsman, D. G. (2016) Dual loss of the SWI/SNF complex ATPases SMARCA4/BRG1 and SMARCA2/BRM is highly sensitive and specific for small cell carcinoma of the ovary, hypercalcaemic type. *J Pathol* **238**, 389-400
18. Patibandla, J. R., Fehniger, J. E., Levine, D. A., and Jelinic, P. (2018) Small cell cancers of the female genital tract: Molecular and clinical aspects. *Gynecol Oncol* **149**, 420-427
19. Jones, S., Wang, T. L., Shih, Ie, M., Mao, T. L., Nakayama, K., Roden, R., Glas, R., Slamon, D., Diaz, L. A., Jr., Vogelstein, B., Kinzler, K. W., Velculescu, V. E., and Papadopoulos, N. (2010) Frequent mutations of chromatin remodeling gene ARID1A in ovarian clear cell carcinoma. *Science* **330**, 228-231
20. Mabuchi, S., Sugiyama, T., and Kimura, T. (2016) Clear cell carcinoma of the ovary: molecular insights and future therapeutic perspectives. *J Gynecol Oncol* **27**, e31
21. del Carmen, M. G., Birrer, M., and Schorge, J. O. (2012) Clear cell carcinoma of the ovary: a review of the literature. *Gynecol Oncol* **126**, 481-490
22. Qin, Q., Ajewole, V. B., Sheu, T. G., Donohue, R., and Singh, M. (2018) Successful treatment of a stage IIIC small-cell carcinoma of the ovary hypercalcaemic subtype using multi-modality therapeutic approach. *Ecancermedicalscience* **12**, 832
23. Young, R. H., Oliva, E., and Scully, R. E. (1994) Small cell carcinoma of the ovary, hypercalcaemic type. A clinicopathological analysis of 150 cases. *Am J Surg Pathol* **18**, 1102-1116
24. Mayes, K., Qiu, Z., Alhazmi, A., and Landry, J. W. (2014) ATP-dependent chromatin remodeling complexes as novel targets for cancer therapy. *Adv Cancer Res* **121**, 183-233
25. Hoffman, G. R., Rahal, R., Buxton, F., Xiang, K., McAllister, G., Frias, E., Bagdasarian, L., Huber, J., Lindeman, A., Chen, D., Romero, R., Ramadan, N., Phadke, T., Haas, K., Jaskelioff, M., Wilson, B. G., Meyer, M. J., Saenz-Vash, V., Zhai, H., Myer, V. E., Porter, J. A., Keen, N., McLaughlin, M. E., Mickanin, C., Roberts, C. W., Stegmeier, F., and Jagani, Z. (2014) Functional epigenetics approach identifies BRM/SMARCA2 as a critical synthetic lethal target in BRG1-deficient cancers. *Proc Natl Acad Sci U S A* **111**, 3128-3133
26. Oike, T., Ogiwara, H., Tominaga, Y., Ito, K., Ando, O., Tsuta, K., Mizukami, T., Shimada, Y., Isomura, H., Komachi, M., Furuta, K., Watanabe, S., Nakano, T., Yokota, J., and Kohno, T. (2013) A synthetic lethality-based strategy to treat cancers harboring a genetic deficiency in the chromatin remodeling factor BRG1. *Cancer Res* **73**, 5508-5518
27. Romero, O. A., Torres-Diz, M., Pros, E., Savola, S., Gomez, A., Moran, S., Saez, C., Iwakawa, R., Villanueva, A., Montuenga, L. M., Kohno, T., Yokota, J., and Sanchez-Cespedes, M. (2014) MAX inactivation in small cell lung cancer disrupts MYC-SWI/SNF programs and is synthetic lethal with BRG1. *Cancer Discov* **4**, 292-303
28. Caumanns, J. J., Wisman, G. B. A., Berns, K., van der Zee, A. G. J., and de Jong, S. (2018) ARID1A mutant ovarian clear cell carcinoma: A clear target for synthetic lethal strategies. *Biochim Biophys Acta Rev Cancer* **1870**, 176-184

29. Lang, J. D., Hendricks, W. P. D., Orlando, K. A., Yin, H., Kiefer, J., Ramos, P., Sharma, R., Pirrotte, P., Raupach, E. A., Sereduk, C., Tang, N., Liang, W. S., Washington, M., Facista, S. J., Zismann, V. L., Cousins, E. M., Major, M. B., Wang, Y., Karnezis, A. N., Sekulic, A., Hass, R., Vanderhyden, B. C., Nair, P., Weissman, B. E., Huntsman, D. G., and Trent, J. M. (2018) Ponatinib Shows Potent Antitumor Activity in Small Cell Carcinoma of the Ovary Hypercalcemic Type (SCCOHT) through Multikinase Inhibition. *Clin Cancer Res* **24**, 1932-1943
30. Chan-Penebre, E., Armstrong, K., Drew, A., Grassian, A. R., Feldman, I., Knutson, S. K., Kuplast-Barr, K., Roche, M., Campbell, J., Ho, P., Copeland, R. A., Chesworth, R., Smith, J. J., Keilhack, H., and Ribich, S. A. (2017) Selective Killing of SMARCA2- and SMARCA4-deficient Small Cell Carcinoma of the Ovary, Hypercalcemic Type Cells by Inhibition of EZH2: In Vitro and In Vivo Preclinical Models. *Mol Cancer Ther* **16**, 850-860
31. Kim, K. H., Kim, W., Howard, T. P., Vazquez, F., Tsherniak, A., Wu, J. N., Wang, W., Haswell, J. R., Walensky, L. D., Hahn, W. C., Orkin, S. H., and Roberts, C. W. (2015) SWI/SNF-mutant cancers depend on catalytic and non-catalytic activity of EZH2. *Nat Med* **21**, 1491-1496
32. Wang, Y., Chen, S. Y., Karnezis, A. N., Colborne, S., Santos, N. D., Lang, J. D., Hendricks, W. P., Orlando, K. A., Yap, D., Kommoss, F., Bally, M. B., Morin, G. B., Trent, J. M., Weissman, B. E., and Huntsman, D. G. (2017) The histone methyltransferase EZH2 is a therapeutic target in small cell carcinoma of the ovary, hypercalcaemic type. *J Pathol* **242**, 371-383
33. Wang, Y., Chen, S. Y., Colborne, S., Lambert, G., Shin, C. Y., Santos, N. D., Orlando, K. A., Lang, J. D., Hendricks, W. P. D., Bally, M. B., Karnezis, A. N., Hass, R., Underhill, T. M., Morin, G. B., Trent, J. M., Weissman, B. E., and Huntsman, D. G. (2018) Histone Deacetylase Inhibitors Synergize with Catalytic Inhibitors of EZH2 to Exhibit Antitumor Activity in Small Cell Carcinoma of the Ovary, Hypercalcemic Type. *Mol Cancer Ther* **17**, 2767-2779
34. Shorstova, T., Marques, M., Su, J., Johnston, J., Kleinman, C. L., Hamel, N., Huang, S., Alaoui-Jamali, M. A., Foulkes, W. D., and Witcher, M. (2019) SWI/SNF-Compromised Cancers Are Susceptible to Bromodomain Inhibitors. *Cancer Res* **79**, 2761-2774
35. Xue, Y., Meehan, B., Fu, Z., Wang, X. Q. D., Fiset, P. O., Rieker, R., Levins, C., Kong, T., Zhu, X., Morin, G., Skeritt, L., Herpel, E., Venneti, S., Martinez, D., Judkins, A. R., Jung, S., Camilleri-Broet, S., Gonzalez, A. V., Guiot, M. C., Lockwood, W. W., Spicer, J. D., Agaimy, A., Pastor, W. A., Dostie, J., Rak, J., Foulkes, W. D., and Huang, S. (2019) SMARCA4 loss is synthetic lethal with CDK4/6 inhibition in non-small cell lung cancer. *Nat Commun* **10**, 557
36. Xue, Y., Meehan, B., Macdonald, E., Venneti, S., Wang, X. Q. D., Witkowski, L., Jelinic, P., Kong, T., Martinez, D., Morin, G., Firlit, M., Abedini, A., Johnson, R. M., Cencic, R., Patibandla, J., Chen, H., Papadakis, A. I., Auguste, A., de Rink, I., Kerkhoven, R. M., Bertos, N., Gotlieb, W. H., Clarke, B. A., Leary, A., Witcher, M., Guiot, M. C., Pelletier, J., Dostie, J., Park, M., Judkins, A. R., Hass, R., Levine, D. A., Rak, J., Vanderhyden, B., Foulkes, W. D., and Huang, S. (2019) CDK4/6 inhibitors target SMARCA4-determined cyclin D1 deficiency in hypercalcemic small cell carcinoma of the ovary. *Nat Commun* **10**, 558
37. Miao, D., Margolis, C. A., Gao, W., Voss, M. H., Li, W., Martini, D. J., Norton, C., Bosse, D., Wankowicz, S. M., Cullen, D., Horak, C., Wind-Rotolo, M., Tracy, A., Giannakis, M., Hodi, F. S., Drake, C. G., Ball, M. W., Allaf, M. E., Snyder, A., Hellmann, M. D., Ho, T., Motzer, R. J., Signoretti, S., Kaelin, W. G., Jr., Choueiri, T. K., and Van Allen, E. M. (2018) Genomic correlates of response to immune checkpoint therapies in clear cell renal cell carcinoma. *Science* **359**, 801-806

38. Motzer, R. J., Tannir, N. M., McDermott, D. F., Aren Frontera, O., Melichar, B., Choueiri, T. K., Plimack, E. R., Barthelemy, P., Porta, C., George, S., Powles, T., Donskov, F., Neiman, V., Kollmannsberger, C. K., Salman, P., Gurney, H., Hawkins, R., Ravaud, A., Grimm, M. O., Bracarda, S., Barrios, C. H., Tomita, Y., Castellano, D., Rini, B. I., Chen, A. C., Mekan, S., McHenry, M. B., Wind-Rotolo, M., Doan, J., Sharma, P., Hammers, H. J., Escudier, B., and CheckMate, I. (2018) Nivolumab plus Ipilimumab versus Sunitinib in Advanced Renal-Cell Carcinoma. *N Engl J Med* **378**, 1277-1290
39. Pan, D., Kobayashi, A., Jiang, P., Ferrari de Andrade, L., Tay, R. E., Luoma, A. M., Tsoucas, D., Qiu, X., Lim, K., Rao, P., Long, H. W., Yuan, G. C., Doench, J., Brown, M., Liu, X. S., and Wucherpfennig, K. W. (2018) A major chromatin regulator determines resistance of tumor cells to T cell-mediated killing. *Science* **359**, 770-775
40. Jelinic, P., Ricca, J., Van Oudenhove, E., Olvera, N., Merghoub, T., Levine, D. A., and Zamarin, D. (2018) Immune-Active Microenvironment in Small Cell Carcinoma of the Ovary, Hypercalcemic Type: Rationale for Immune Checkpoint Blockade. *J Natl Cancer Inst* **110**, 787-790
41. Fukumoto, T., Fatkhutdinov, N., Zundell, J. A., Tcyganov, E. N., Nacarelli, T., Karakashev, S., Wu, S., Liu, Q., Gabrilovich, D. I., and Zhang, R. (2019) HDAC6 Inhibition Synergizes with Anti-PD-L1 Therapy in ARID1A-Inactivated Ovarian Cancer. *Cancer Res* **79**, 5482-5489
42. Hamanishi, J., Mandai, M., Ikeda, T., Minami, M., Kawaguchi, A., Murayama, T., Kanai, M., Mori, Y., Matsumoto, S., Chikuma, S., Matsumura, N., Abiko, K., Baba, T., Yamaguchi, K., Ueda, A., Hosoe, Y., Morita, S., Yokode, M., Shimizu, A., Honjo, T., and Konishi, I. (2015) Safety and Antitumor Activity of Anti-PD-1 Antibody, Nivolumab, in Patients With Platinum-Resistant Ovarian Cancer. *J Clin Oncol* **33**, 4015-4022
43. Ambrosio, S., Sacca, C. D., Amente, S., Paladino, S., Lania, L., and Majello, B. (2017) Lysine-specific demethylase LSD1 regulates autophagy in neuroblastoma through SESN2-dependent pathway. *Oncogene* **36**, 6701-6711
44. Amente, S., Lania, L., and Majello, B. (2013) The histone LSD1 demethylase in stemness and cancer transcription programs. *Biochim Biophys Acta* **1829**, 981-986
45. Schulte, J. H., Lim, S., Schramm, A., Friedrichs, N., Koster, J., Versteeg, R., Ora, I., Pajtler, K., Klein-Hitpass, L., Kuhfittig-Kulle, S., Metzger, E., Schule, R., Eggert, A., Buettner, R., and Kirfel, J. (2009) Lysine-specific demethylase 1 is strongly expressed in poorly differentiated neuroblastoma: implications for therapy. *Cancer Res* **69**, 2065-2071
46. Huang, J., Sengupta, R., Espejo, A. B., Lee, M. G., Dorsey, J. A., Richter, M., Opravil, S., Shiekhata, R., Bedford, M. T., Jenuwein, T., and Berger, S. L. (2007) p53 is regulated by the lysine demethylase LSD1. *Nature* **449**, 105-108
47. Kontaki, H., and Talianidis, I. (2010) Cross-talk between post-translational modifications regulate life or death decisions by E2F1. *Cell Cycle* **9**, 3836-3837
48. Kontaki, H., and Talianidis, I. (2010) Lysine methylation regulates E2F1-induced cell death. *Mol Cell* **39**, 152-160
49. Scoumanne, A., and Chen, X. (2007) The lysine-specific demethylase 1 is required for cell proliferation in both p53-dependent and -independent manners. *J Biol Chem* **282**, 15471-15475
50. Wang, J., Hevi, S., Kurash, J. K., Lei, H., Gay, F., Bajko, J., Su, H., Sun, W., Chang, H., Xu, G., Gaudet, F., Li, E., and Chen, T. (2009) The lysine demethylase LSD1 (KDM1) is required for maintenance of global DNA methylation. *Nat Genet* **41**, 125-129
51. Sheng, W., LaFleur, M. W., Nguyen, T. H., Chen, S., Chakravarthy, A., Conway, J. R., Li, Y., Chen, H., Yang, H., Hsu, P. H., Van Allen, E. M., Freeman, G. J., De Carvalho, D. D., He, H. H., Sharpe, A. H., and Shi, Y. (2018) LSD1 Ablation Stimulates Anti-tumor Immunity and Enables Checkpoint Blockade. *Cell* **174**, 549-563 e519

52. Chen, S., Lee, L. F., Fisher, T. S., Jessen, B., Elliott, M., Evering, W., Logronio, K., Tu, G. H., Tsaparikos, K., Li, X., Wang, H., Ying, C., Xiong, M., VanArsdale, T., and Lin, J. C. (2015) Combination of 4-1BB agonist and PD-1 antagonist promotes antitumor effector/memory CD8 T cells in a poorly immunogenic tumor model. *Cancer Immunol Res* **3**, 149-160
53. Juneja, V. R., McGuire, K. A., Manguso, R. T., LaFleur, M. W., Collins, N., Haining, W. N., Freeman, G. J., and Sharpe, A. H. (2017) PD-L1 on tumor cells is sufficient for immune evasion in immunogenic tumors and inhibits CD8 T cell cytotoxicity. *J Exp Med* **214**, 895-904
54. Hiramatsu, H., Kobayashi, K., Kobayashi, K., Haraguchi, T., Ino, Y., Todo, T., and Iba, H. (2017) The role of the SWI/SNF chromatin remodeling complex in maintaining the stemness of glioma initiating cells. *Sci Rep* **7**, 889
55. Rossbach, M. (2011) Non-Coding RNAs in Neural Networks, REST-Assured. *Front Genet* **2**, 8
56. Nacht, A. S., Pohl, A., Zaurin, R., Soronellas, D., Quilez, J., Sharma, P., Wright, R. H., Beato, M., and Vicent, G. P. (2016) Hormone-induced repression of genes requires BRG1-mediated H1.2 deposition at target promoters. *EMBO J* **35**, 1822-1843
57. Yatim, A., Benne, C., Sobhian, B., Laurent-Chabalier, S., Deas, O., Judde, J. G., Lelievre, J. D., Levy, Y., and Benkirane, M. (2012) NOTCH1 nuclear interactome reveals key regulators of its transcriptional activity and oncogenic function. *Mol Cell* **48**, 445-458
58. Cerami, E., Gao, J., Dogrusoz, U., Gross, B. E., Sumer, S. O., Aksoy, B. A., Jacobsen, A., Byrne, C. J., Heuer, M. L., Larsson, E., Antipin, Y., Reva, B., Goldberg, A. P., Sander, C., and Schultz, N. (2012) The cBio cancer genomics portal: an open platform for exploring multidimensional cancer genomics data. *Cancer Discov* **2**, 401-404
59. Gao, J., Aksoy, B. A., Dogrusoz, U., Dresdner, G., Gross, B., Sumer, S. O., Sun, Y., Jacobsen, A., Sinha, R., Larsson, E., Cerami, E., Sander, C., and Schultz, N. (2013) Integrative analysis of complex cancer genomics and clinical profiles using the cBioPortal. *Sci Signal* **6**, pl1
60. Qin, Y., Vasilatos, S. N., Chen, L., Wu, H., Cao, Z., Fu, Y., Huang, M., Vlad, A. M., Lu, B., Oesterreich, S., Davidson, N. E., and Huang, Y. (2019) Inhibition of histone lysine-specific demethylase 1 elicits breast tumor immunity and enhances antitumor efficacy of immune checkpoint blockade. *Oncogene* **38**, 390-405
61. Bally, A. P., Austin, J. W., and Boss, J. M. (2016) Genetic and Epigenetic Regulation of PD-1 Expression. *J Immunol* **196**, 2431-2437
62. Chi, T. (2004) A BAF-centred view of the immune system. *Nat Rev Immunol* **4**, 965-977
63. Ni, Z., Karaskov, E., Yu, T., Callaghan, S. M., Der, S., Park, D. S., Xu, Z., Pattenden, S. G., and Bremner, R. (2005) Apical role for BRG1 in cytokine-induced promoter assembly. *Proc Natl Acad Sci U S A* **102**, 14611-14616
64. Shen, J., Ju, Z., Zhao, W., Wang, L., Peng, Y., Ge, Z., Nagel, Z. D., Zou, J., Wang, C., Kapoor, P., Ma, X., Ma, D., Liang, J., Song, S., Liu, J., Samson, L. D., Ajani, J. A., Li, G. M., Liang, H., Shen, X., Mills, G. B., and Peng, G. (2018) ARID1A deficiency promotes mutability and potentiates therapeutic antitumor immunity unleashed by immune checkpoint blockade. *Nat Med* **24**, 556-562
65. Naito, T., Umemura, S., Nakamura, H., Zenke, Y., Udagawa, H., Kirita, K., Matsumoto, S., Yoh, K., Niho, S., Motoi, N., Aokage, K., Tsuboi, M., Ishii, G., and Goto, K. (2019) Successful treatment with nivolumab for SMARCA4-deficient non-small cell lung carcinoma with a high tumor mutation burden: A case report. *Thorac Cancer* **10**, 1285-1288
66. Xia, T., Konno, H., Ahn, J., and Barber, G. N. (2016) Deregulation of STING Signaling in Colorectal Carcinoma Constrains DNA Damage Responses and Correlates With Tumorigenesis. *Cell Rep* **14**, 282-297

67. Curtis, B. J., Zraly, C. B., Marenda, D. R., and Dingwall, A. K. (2011) Histone lysine demethylases function as co-repressors of SWI/SNF remodeling activities during *Drosophila* wing development. *Dev Biol* **350**, 534-547
68. Hiramatsu, H., Kobayashi, K., Kobayashi, K., Haraguchi, T., Ino, Y., Todo, T., and Iba, H. (2018) Author Correction: The role of the SWI/SNF chromatin remodeling complex in maintaining the stemness of glioma initiating cells. *Sci Rep* **8**, 16079
69. Schiavetti, F., Thonnard, J., Colau, D., Boon, T., and Coulie, P. G. (2002) A human endogenous retroviral sequence encoding an antigen recognized on melanoma by cytolytic T lymphocytes. *Cancer Res* **62**, 5510-5516
70. Improgo, M. R., Soll, L. G., Tapper, A. R., and Gardner, P. D. (2013) Nicotinic acetylcholine receptors mediate lung cancer growth. *Front Physiol* **4**, 251
71. Chiappinelli, K. B., Strissel, P. L., Desrichard, A., Li, H., Henke, C., Akman, B., Hein, A., Rote, N. S., Cope, L. M., Snyder, A., Makarov, V., Budhu, S., Slamon, D. J., Wolchok, J. D., Pardoll, D. M., Beckmann, M. W., Zahnow, C. A., Merghoub, T., Chan, T. A., Baylin, S. B., and Strick, R. (2015) Inhibiting DNA Methylation Causes an Interferon Response in Cancer via dsRNA Including Endogenous Retroviruses. *Cell* **162**, 974-986
72. Le, D. T., Uram, J. N., Wang, H., Bartlett, B. R., Kemberling, H., Eyring, A. D., Skora, A. D., Luber, B. S., Azad, N. S., Laheru, D., Biedrzycki, B., Donehower, R. C., Zaheer, A., Fisher, G. A., Crocenzi, T. S., Lee, J. J., Duffy, S. M., Goldberg, R. M., de la Chapelle, A., Koshiji, M., Bhajee, F., Huebner, T., Hruban, R. H., Wood, L. D., Cuka, N., Pardoll, D. M., Papadopoulos, N., Kinzler, K. W., Zhou, S., Cornish, T. C., Taube, J. M., Anders, R. A., Eshleman, J. R., Vogelstein, B., and Diaz, L. A., Jr. (2015) PD-1 Blockade in Tumors with Mismatch-Repair Deficiency. *N Engl J Med* **372**, 2509-2520
73. Leung, D. C., and Lorincz, M. C. (2012) Silencing of endogenous retroviruses: when and why do histone marks predominate? *Trends Biochem Sci* **37**, 127-133
74. Maksakova, I. A., Mager, D. L., and Reiss, D. (2008) Keeping active endogenous retroviral-like elements in check: the epigenetic perspective. *Cell Mol Life Sci* **65**, 3329-3347
75. Kassiotis, G., and Stoye, J. P. (2016) Immune responses to endogenous retroelements: taking the bad with the good. *Nat Rev Immunol* **16**, 207-219
76. Szpakowski, S., Sun, X., Lage, J. M., Dyer, A., Rubinstein, J., Kowalski, D., Sasaki, C., Costa, J., and Lizardi, P. M. (2009) Loss of epigenetic silencing in tumors preferentially affects primate-specific retroelements. *Gene* **448**, 151-167
77. Sachs, P., Ding, D., Bergmaier, P., Lamp, B., Schlagheck, C., Finkernagel, F., Nist, A., Stiewe, T., and Mermoud, J. E. (2019) SMARCA4 ATPase activity is required to silence endogenous retroviruses in embryonic stem cells. *Nat Commun* **10**, 1335
78. Leruste, A., Tosello, J., Ramos, R. N., Tauziède-Espariat, A., Brohard, S., Han, Z. Y., Beccaria, K., Andrianteranagna, M., Caudana, P., Nikolic, J., Chauvin, C., Niborski, L. L., Manriquez, V., Richer, W., Masliah-Planchon, J., Grossetete-Lalami, S., Bohec, M., Lameiras, S., Baulande, S., Pouponnot, C., Coulomb, A., Galmiche, L., Surdez, D., Servant, N., Helft, J., Sedlik, C., Puget, S., Benaroch, P., Delattre, O., Waterfall, J. J., Piaggio, E., and Bourdeaut, F. (2019) Clonally Expanded T Cells Reveal Immunogenicity of Rhabdoid Tumors. *Cancer Cell* **36**, 597-612 e598
79. Macfarlan, T. S., Gifford, W. D., Agarwal, S., Driscoll, S., Lettieri, K., Wang, J., Andrews, S. E., Franco, L., Rosenfeld, M. G., Ren, B., and Pfaff, S. L. (2011) Endogenous retroviruses and neighboring genes are coordinately repressed by LSD1/KDM1A. *Genes Dev* **25**, 594-607

## Legends

**Figure 1: (A)** TCGA analysis for LSD1 expression in different human cancers. **(B)** TCGA analysis for LSD1 expression in SWI/SNF-mutated tumors. **Table 1:** Cytotoxicity of SP-2577 and SP-2513 in SWI/SNF-mutated cancer cell lines. **Table 2:** Inhibition of LSD1 enzymatic activity of SP-2577 and SP-2513.

**Figure 2: (A)** qPCR analysis of SCCOHT cell lines BIN67, COV434 and SCCOHT-1 after 72h of SP-2577 treatment showing increased expression of ERVs and IFN pathway cytokines. **(B)** MSD panel of chemokines and cytokines from SCCOHT COV434 cell conditioned media in the presence or absence of SP-2577 for 72h. \*= $p < 0.05$ , \*\*= $p < 0.01$ .

**Figure 3: (A)** Immune infiltration assay in SCCOHT organoids imaging analysis. COV434, BIN67 and SCCOHT-1 derived- organoids were incubated with conditioned medium pretreated with 3  $\mu$ M SP-2577, SP-2513 or DMSO in the presence of RFP-tagged PBMCs. After 48h the levels of lymphocyte infiltration were measured by z-stack analysis by Cytation 5 imaging. P values for COV434= $<0.0001$ , BIN67 = 0.0016, and SCCOHT-1 = 0.0196. Right panel: Experimental design **(B)** IF analysis: RFP-tagged lymphocytes infiltration in SCCOHT organoids micro sections was assessed by analysis of RFP levels on confocal scope after 48h co-culture in presence of SP-2577 or SP-2513 conditioned medium. **(C)** Immune infiltration assay of COV434 cells treated with increased concentration of SP-2577 for 48h. The levels of lymphocytes infiltration correlate with SP-2577 dose.

**Figure 4: (A)** RT-PCR analysis of COV434 cells after SP-2577 treatment shows increase of PD-1 and PD-L1 expression levels, which are lost after Doxycycline treatment. **(B)** Co-treatment of SCCOHT organoids with SP-2577 and anti PD-L1 antibodies and lymphocytes treated with anti CTLA-4 antibodies showed an increase in lymphocyte infiltration as checked after 48h.

**Figure 5: (A)** Densitometry analysis of western blot for SMARCA4 expression level in COV434 pIND20 BRG1-2.7 after 1 $\mu$ M Doxycycline daily treatment (D=days) **(B)** RT-PCR for BRG1 and BRM expression levels in COV434 pIND20 BRG1-2.7. Both gene expression increased after SP-2577 treatment. **(C)** The levels of lymphocyte infiltration are significantly reduced after SMARCA4 re-expression in COV434 pIND20 BRG1-2.7 (P value = 0.038). **(D)** RT-PCR analysis of SMARCA4-induced COV434 pIND20 BRG1-2.7 after 72h SP2577 treatment shows decrease of ERVs activity and INF expression. **(E)** RT-PCR analysis of COV434 cells after SP-2577 treatment shows increase of PD-L1 expression levels, which are lost after Doxycycline treatment **(F)** MSD analysis of SMARCA4-induced COV434 pIND20 BRG1-2.7 after 72h SP-2577 treatment shows significant decrease of cyto/chemokines released in medium after treatment. **(G)** Treatment of SMARCA4-induced COV434 pIND20 BRG1-2.7 organoids with conditioned medium (CM) from SMARCA4-deficient COV434 pIND20 BRG1-2.7 does not affect lymphocyte infiltration suggesting SMARCA4 plays role in immune response. Left panel: Experimental design.

**Figure 6: (A)** level of lymphocytes infiltration is dependent of SP-2577 treatment in TOV21G pIND20-ARID1A cells line. **(B)** lymphocytes infiltration is significantly reduced in TOV21G

pIND20-ARID1A cells after ARID1A re-expression upon Doxycycline treatment (P value = 0.004).  
**(C)** co-treatment of SP-2577 and CTLA-4 antibodies in the immune infiltration assay showed an increase in lymphocyte infiltration in TOV21G-pIND20-ARID1A after 48h

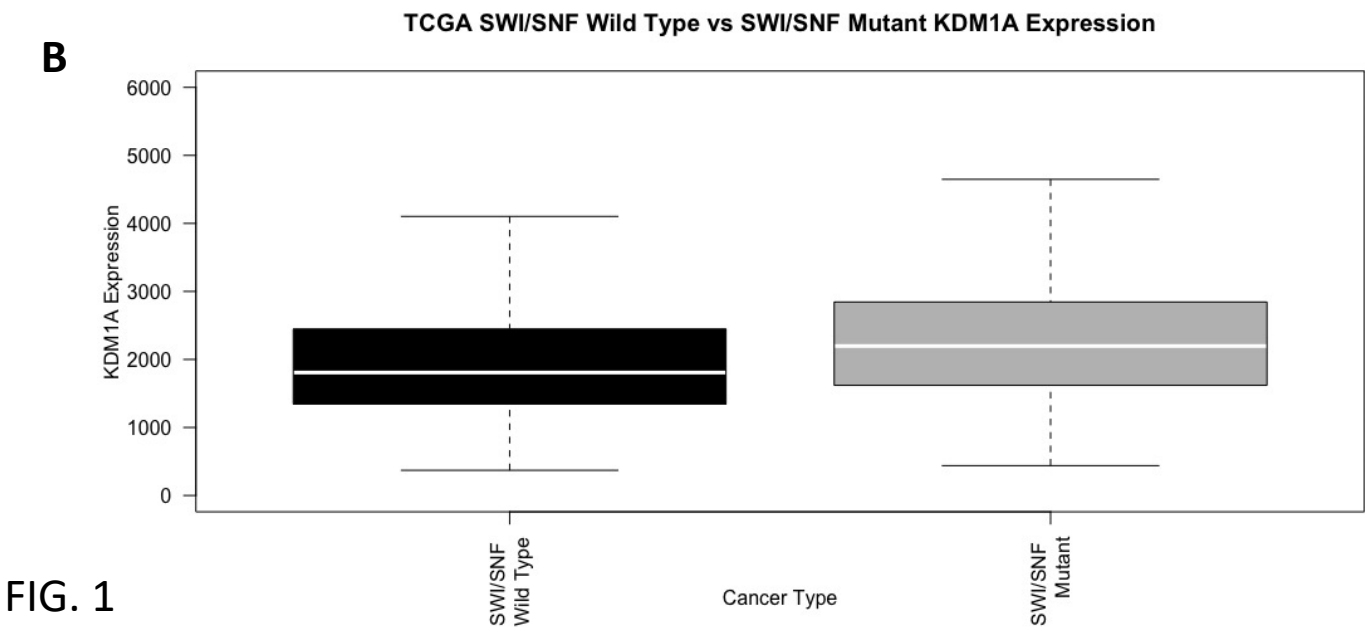
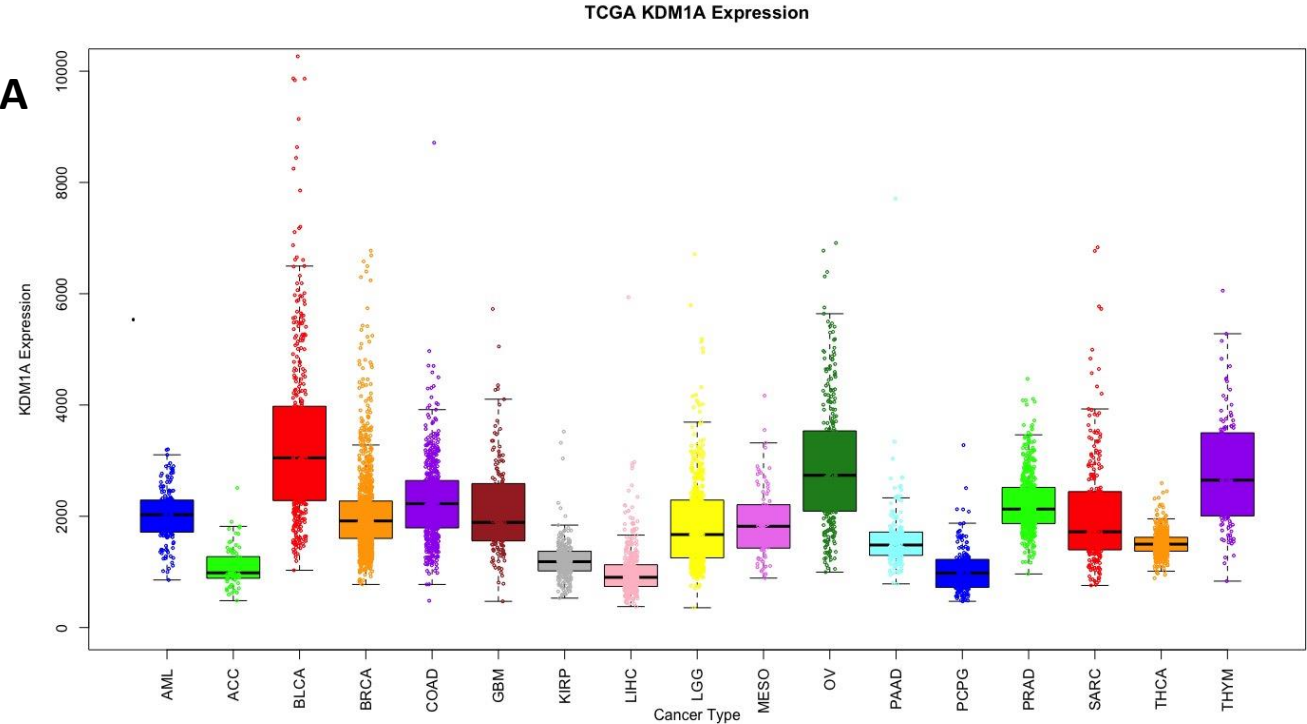


Table 1				
Cell line	Cancer type	Drug IC <sub>50</sub> (μM)		SWI/SNF mutation
		SP-2577	SP-2513	
COV434	SCCOHT	0.529	9.985	SMARCA4
BIN67	SCCOHT	0.417	10	SMARCA4
SCCOHT-1	SCCOHT	1.098	3.65	SMARCA4
TOV21G	OCCC	0.203	24.54	ARID1A
SKOV3	Ovary ADC	0.013	---	SMARCC1
A427	Lung ADC	0.1422	---	SMARCA4
H522	Lung ADC nscl	2.819	---	SMARCA4
A549	Lung ADC	0.248	---	SMARCA4
H1299	Lung ADC nscl	0.212	---	SMARCA4
G401	Kidney Rhabdoid	0.3874	---	SMARCB1
G402	Kidney renal leiomyoblast	1.179	---	SMARCB1
HCC15	CRC	0.117	---	SMARCA4

Table 2	
Drug	IC <sub>50</sub> (μM)
SP-2577	0.013
SP-2513	>1

LSD1 screening biochemical assay

FIG. 1

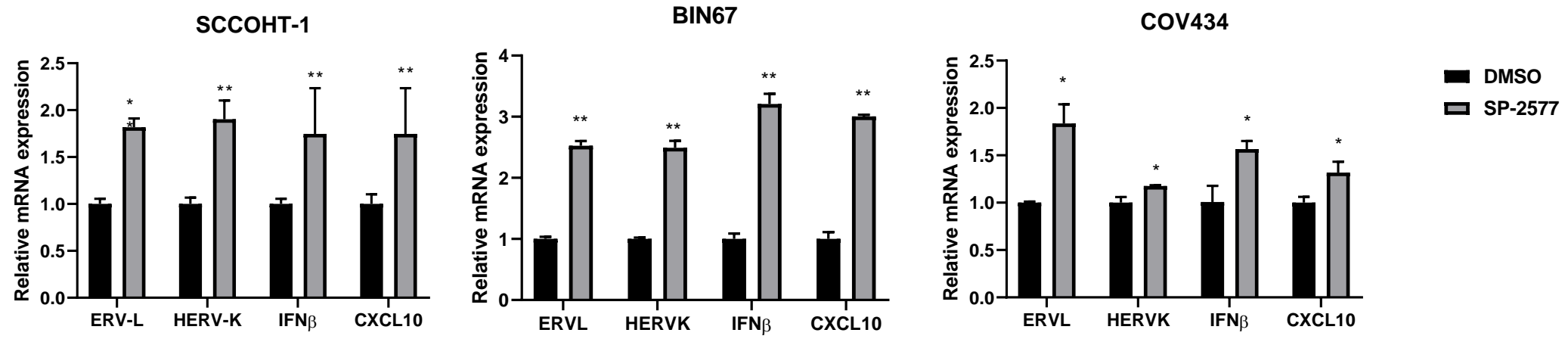
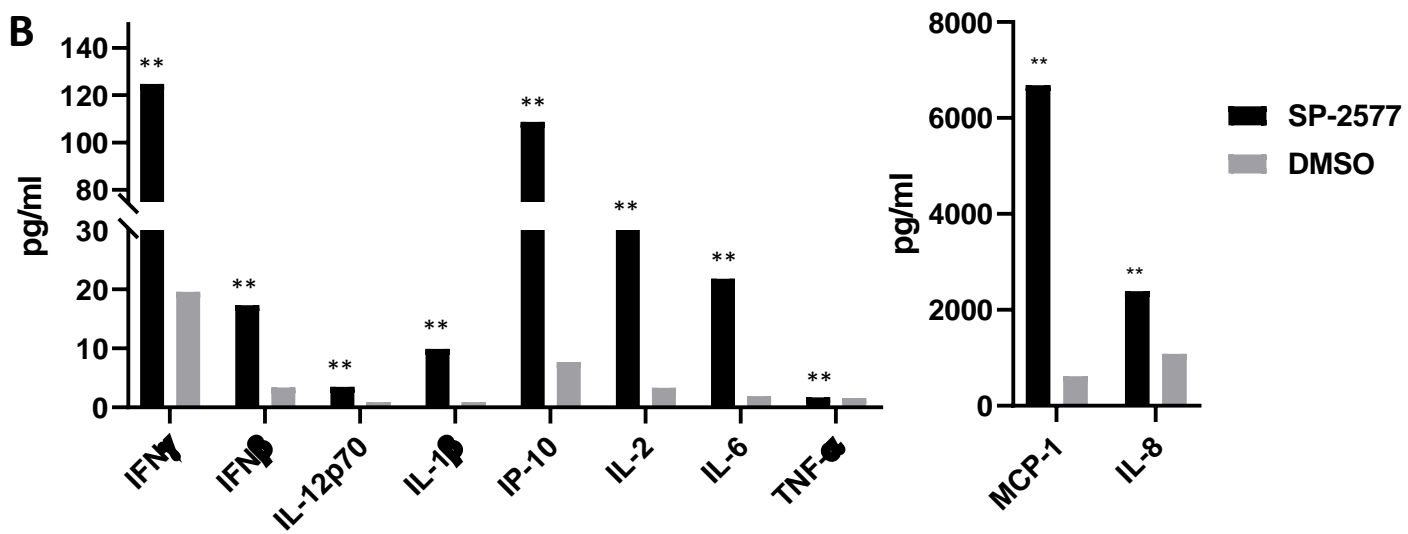
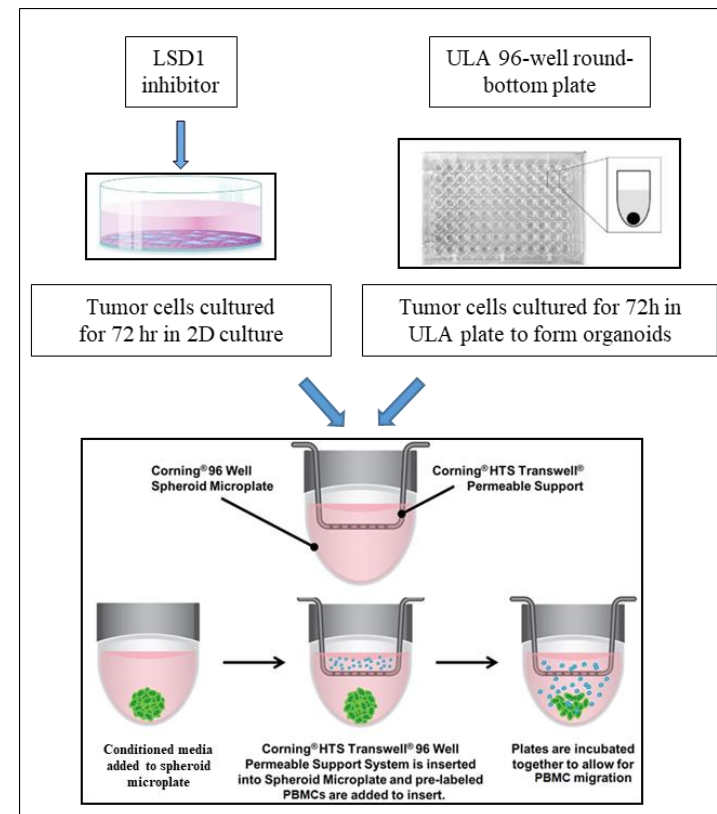
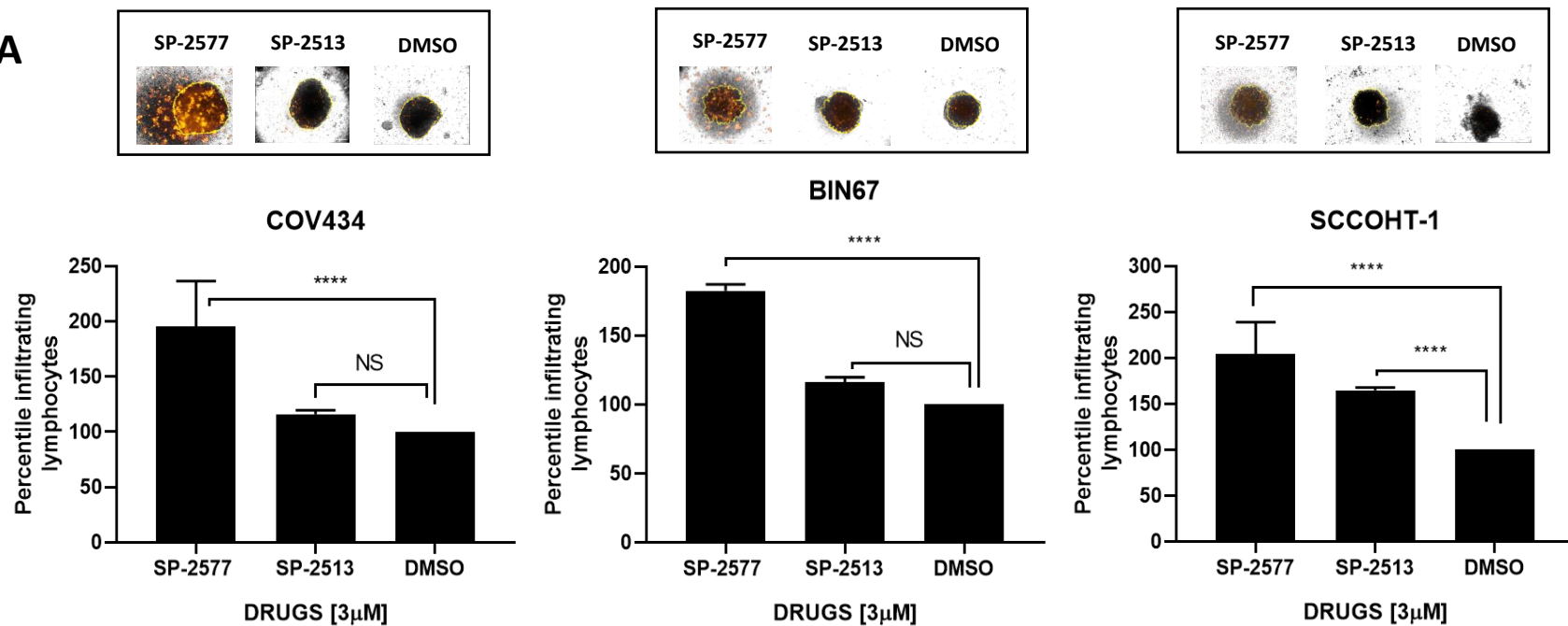
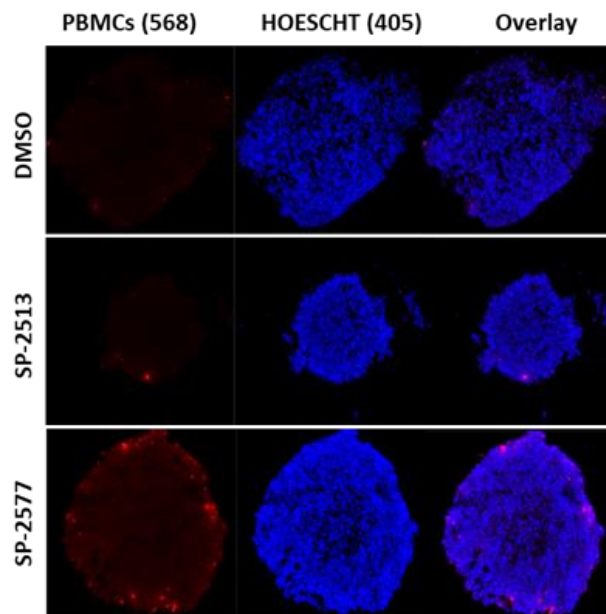
**A****B**

FIG. 2

**A**



**B**



**C**

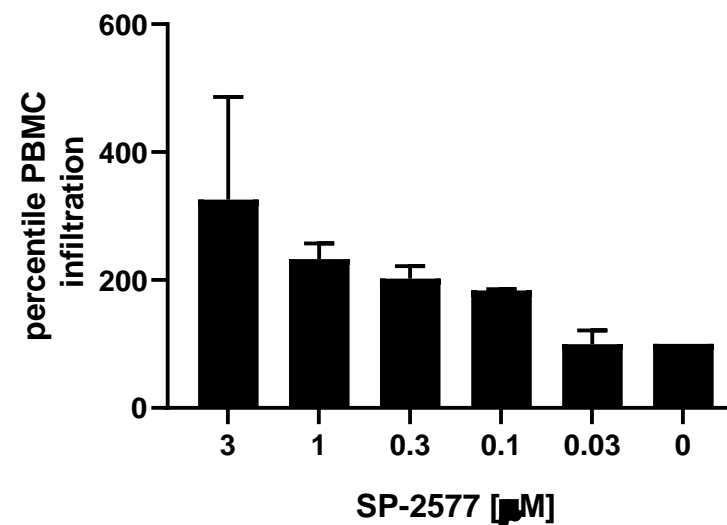


FIG. 3

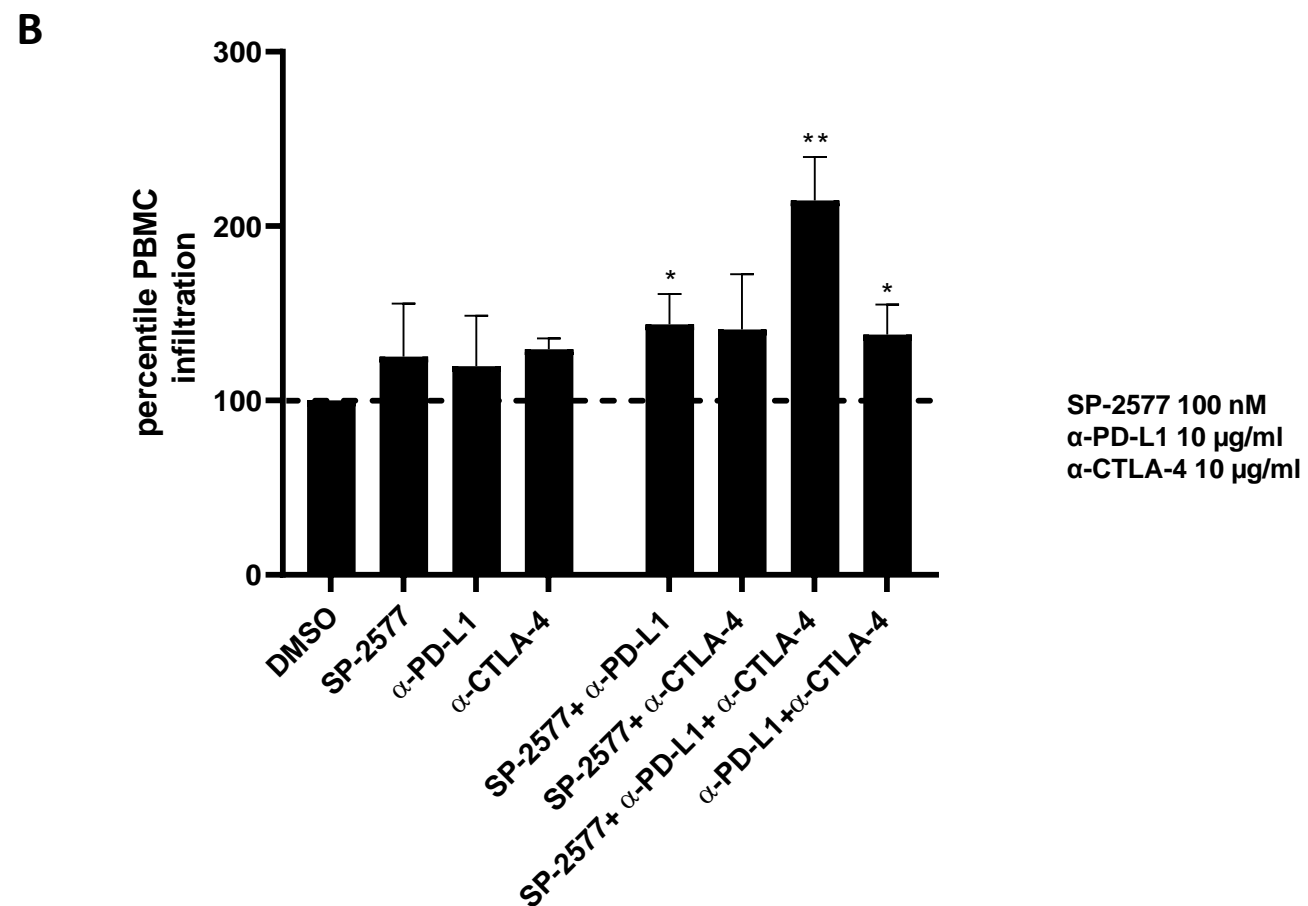
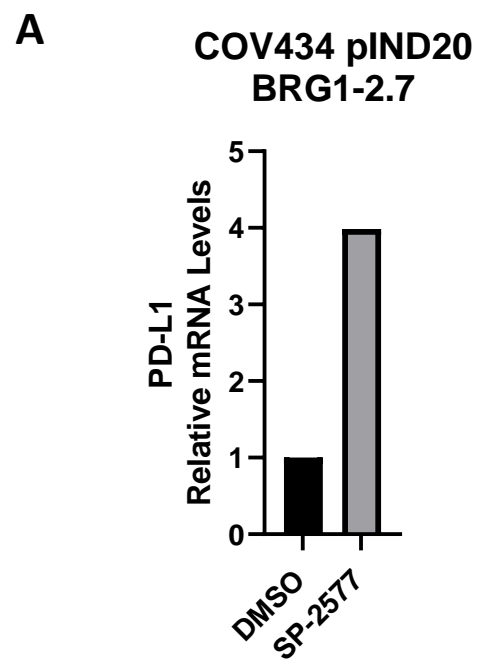
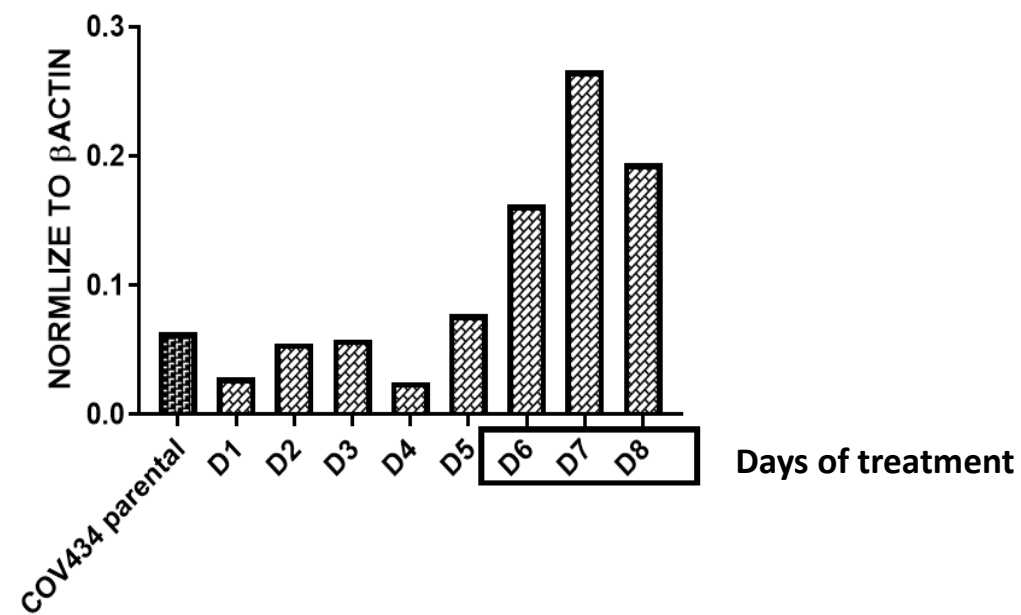
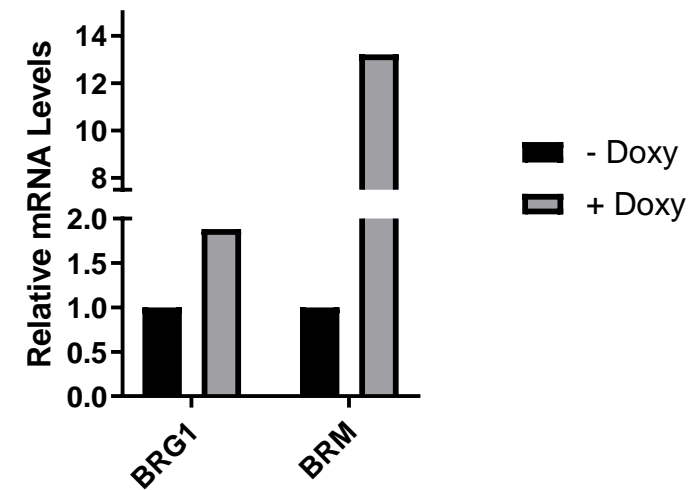


FIG. 4

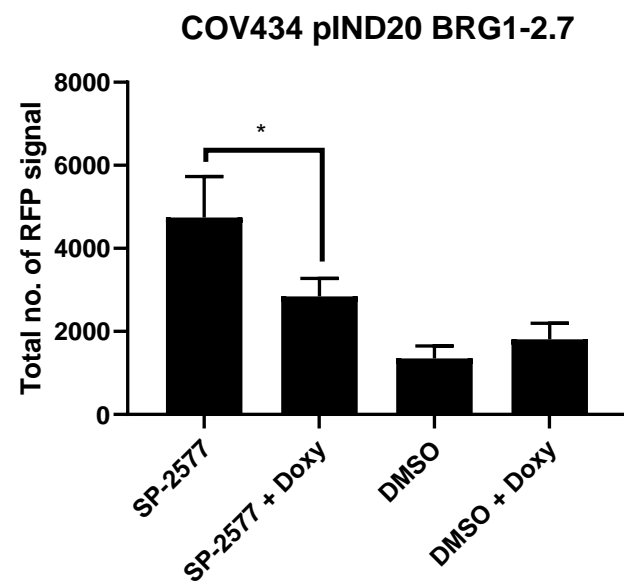
A



B



C



D

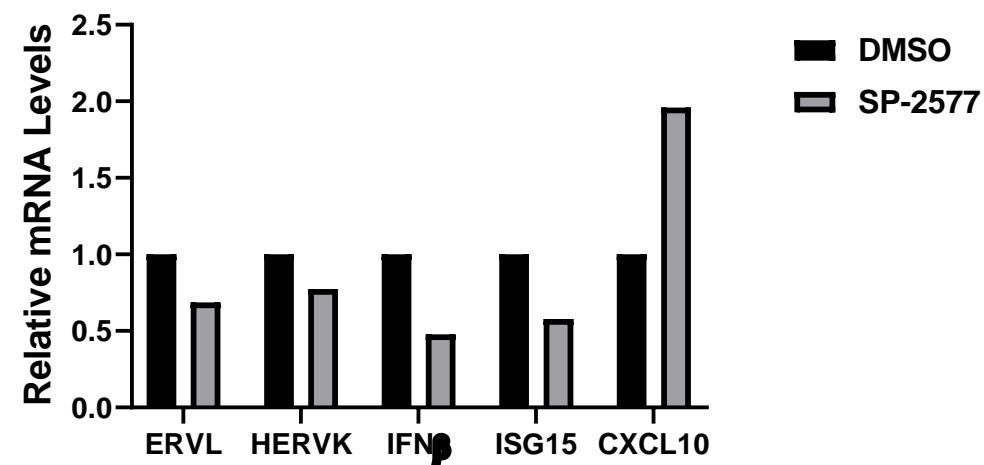
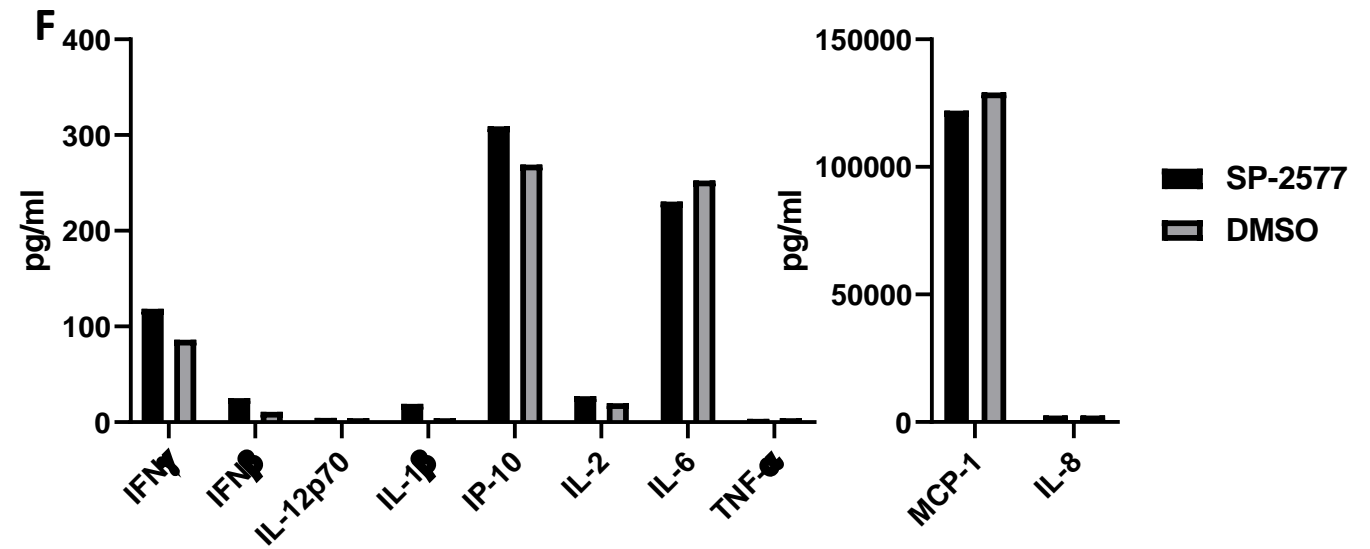
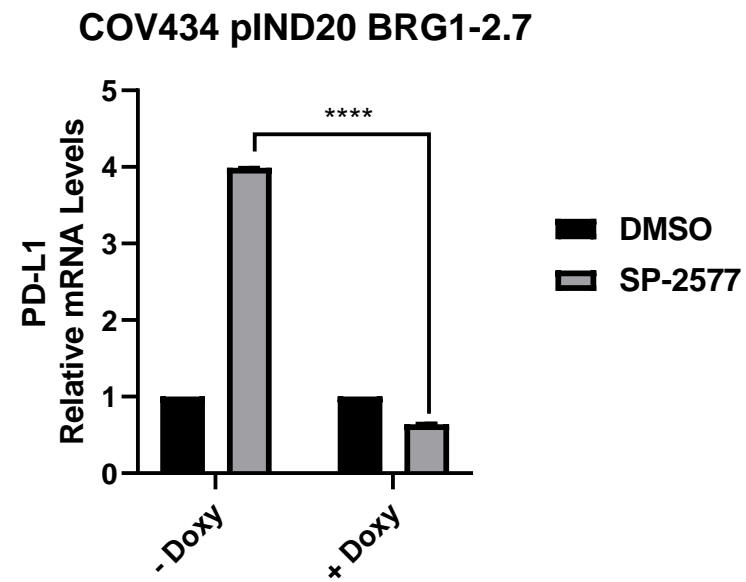


FIG. 5

E



G

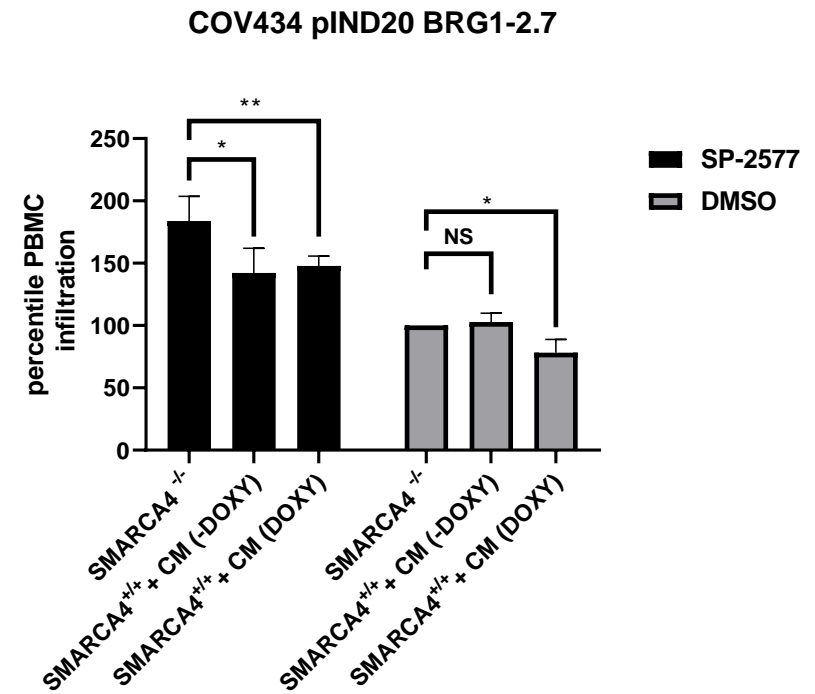
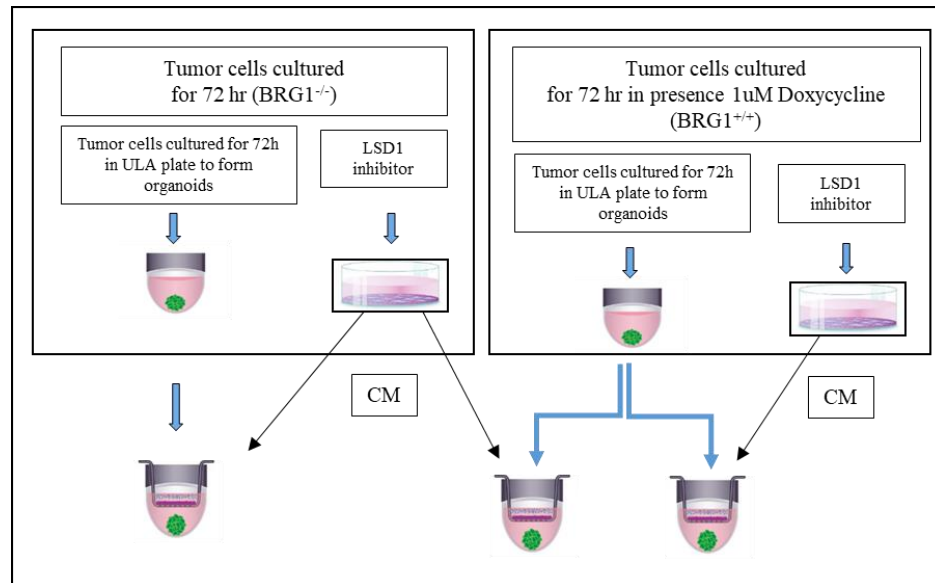
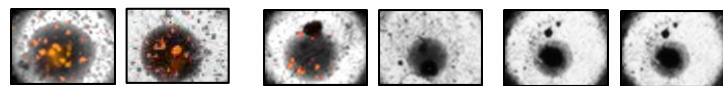
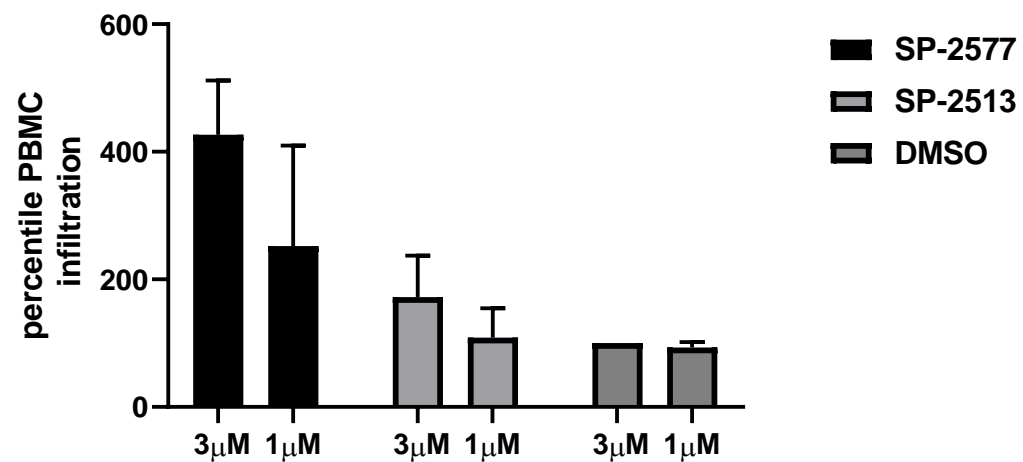


FIG. 5

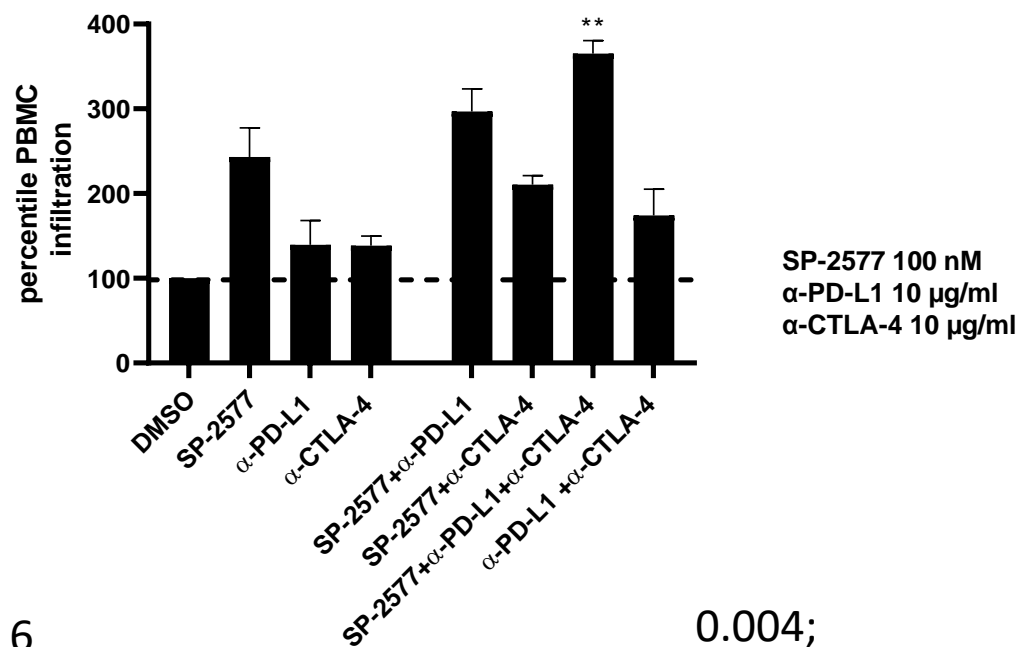
A



## TOV21G-pIND20-ARID1A



C



B

## TOV21G-pIND20-ARID1A

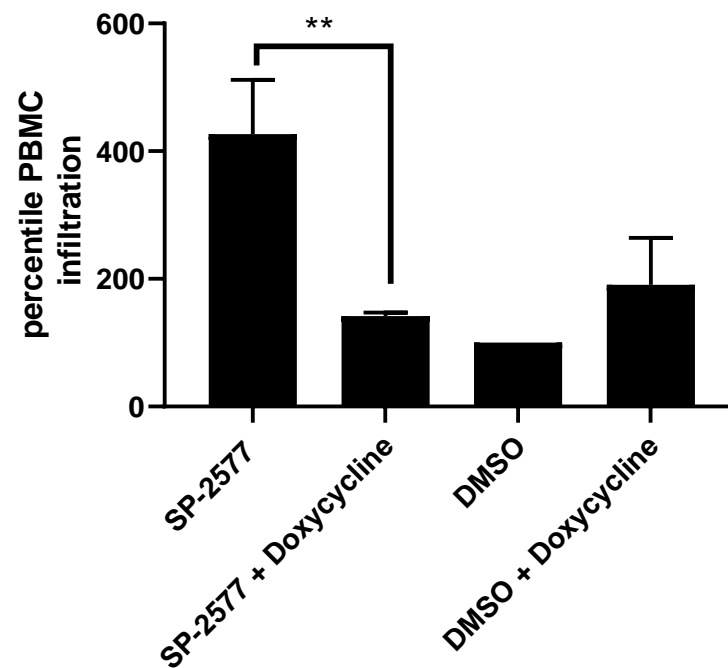


FIG. 6

0.004;